January 2015

The Unique N- And C-Terminal Domains Of Metallothionein-3 Influence The Growth And Differentiation Of Breast Cancer Cells

Brent Jeffrey Voels

Follow this and additional works at: https://commons.und.edu/theses

THE UNIQUE N- AND C-TERMINAL DOMAINS OF METALLOTHIONEIN-3
INFLUENCE THE GROWTH AND DIFFERENTIATION OF BREAST CANCER
CELLS

by

Brent Jeffrey Voels

Bachelor of Arts, Minnesota State University Moorhead, USA 2008

A Dissertation

Submitted to the Graduate Faculty

of the

University of North Dakota

in partial fulfillment of the requirements

for the degree of
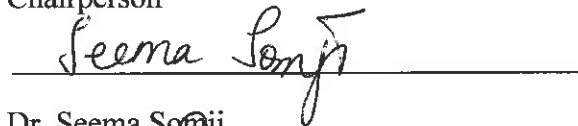
Doctor of Philosophy

Grand Forks, North Dakota

December

2015
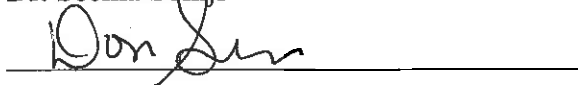
This dissertation, submitted by Brent Jeffrey Voels in partial fulfillment of the requirements for the Doctor of Philosophy Degree from the University of North Dakota, has been read by the Faculty Advisory Committee under whom the work has been done and is approved.

Dr. Scott Garrett,
Chairperson

Dr. Seema Somji

Dr. Donald Sens

Dr. John Shabb

Dr. Van Doze

This dissertation meets the formatting requirements of the Graduate School of the University of North Dakota, and is hereby approved.

Dr. Wayne Swisher,
Dean of the Graduate School

December 7, 2015

Date

PERMISSION

Title: The Unique N- and C-Terminal Domains of Metallothionein-3 Influence the Growth and Differentiation of Breast Cancer Cells

Department: Department of Basic Sciences

Degree: Doctor of Philosophy

In presenting this thesis in partial fulfillment of the requirements for a graduate degree from the University of North Dakota, I agree that the library of the University shall make it freely available for inspection. I further agree that permission for extensive copying for scholarly purposes may be granted by the professor who supervised my dissertation work or in his absence, by the chairperson of the department or the dean of the Graduate School. It is understood that any copying or publication or other use of this dissertation or part thereof for financial gain shall not be allowed without my written permission. It is also understood that due recognition shall be given to me and to the University of North Dakota in any scholarly use which may be made of any material in my dissertation.

Brent Voels
December 3rd 2015

TABLE OF CONTENTS

LIST OF FIGURES

Supplemental Figures

LIST OF TABLES

ACKNOWLEDGEMENTS

I would like to thank Scott Garrett, Seema Somji, and Donald Sens for being excellent and patient mentors through the years. Over the course of my graduate career I have come into to contact with many helpful fellow graduate students and colleagues whose help has been greatly appreciated. None of this would have been possible without the unconditional support from my parents Jeffrey and Beth Voels.

ABSTRACT

Toxic insult from the heavy metal cadmium is known to induce the expression of
metallothioneins (MT) which are cysteine-rich heavy metal binding proteins six to seven
kilodaltons in size. Previous research demonstrates that over-expression of MT-3 occurs
in the majority of breast cancers and is associated with poor patient outcome.
Furthermore, MT-3 has been shown to inhibit the growth of breast cancer and prostate
cancer cell lines. Studies have shown that the MT-3 protein contains 7 additional amino
acids that are not present in any other member of the MT gene family, a 6 amino acid C-
terminal sequence and a Thr in the N-terminal region. The unique N-terminal sequence
is responsible for the growth inhibitory activity of MT-3 in the neuronal system, while
the function of C-terminal region remains unknown. The unique N- and C-terminal
domains of MT-3 may play alternative roles in the differentiation and growth of breast
cancer cells.

One goal of this study was to characterize the function of the N- and C-terminal
domains of MT-3 in the MCF7 breast cancer cell line. For this purpose six different
constructs of MTs were prepared which were as follows: wild type (WT) MT-3, MT-3 N-
terminal site directed mutagenesis (MT-3 P7T P9T), MT-3 C-terminal deletion (MT-3
E55_E60del), WT MT-1E, and MT-1E mutated to contain the N -terminal of MT-3 (MT-
1E N4_C5insTCPCP), or the C-terminal (MT-1E G52_A53insEAAEAE), or both the N-

and the C-terminal of MT-3 (MT-1E N4_C5insTCPCP and G52_A53insEAAEAE).

Each of these constructs was transfected into MCF7 cells. Both the growth rate and the

transepithelial resistance (TER) of each cell line were measured. Growth rates were

statistically significantly reduced in all cell lines except MCF7 parent, Blank Vector, and

MT-1E. Vectorial active transport was increased in WT MT-3 and mutants containing

the C-terminal of MT-3 as indicated by the formation of domes and increased TER.

Observations of confluent cell cultures of mutant cell lines were also performed to

determine the doming phenotype. Doming was observed in cell cultures possessing the

C-terminal region of MT-3, and the WT MT-3 cell line. The data obtained suggests that

the N-terminal region of MT-3 is involved in growth inhibitory activity even in the

absence of the C-terminal domain. The C-terminal region is involved in vectorial active

transport which is indicated by the formation of domes in cell culture. Depending on cell

culture conditions the N-terminal region of MT-3 may attenuate the C-terminal domain's

ability to confer the doming phenotype.

Microarray analysis of the MCF7 mutants was also performed to determine

alterations in gene expression. Overlapping hierarchal clustering demonstrates that the

N- and C-terminal mutants have unique expression relationships. Genes that were

differentially regulated on the microarray and were further validated included the GAGE

family antigens. Several GAGE antigens were investigated to examine differential

expression between the N- and C-terminal of MT-3. These included: GAGE12H,

GAGE12G, GAGE4, GAGE5, GAGE6, GAGE2E-1, GAGE2E-2, GAGE2E-1E, and

GAGE2C. A significant repression of GAGE2C, GAGE2E-1, GAGE2E-2, GAGE5,

GAGE6, and GAGE12H antigen expression was seen in MCF7 mutants NT-1E, WT MT-

3, and MT-3ΔCT. Up regulation of GAG2C, GAGE2E-2, GAGE5, and GAGE12H

antigens occurred in MCF7 mutants MT-1E and CT-1E. The GAGE12G antigen

demonstrated increased expression in only MCF7 mutant cell lines MT-1E, CT-1E, and

MT-3ΔNT. The GAGE6 antigen was the only antigen to show repression in the presence

of the N-terminal of MT-3 and up regulation in the presence of the C-terminal of MT-3

but not in the presence of MT-1E.

In conclusion, this study further characterizes the unique properties of the N- and

the C-terminal domain of MT-3 and the potential role that it may play in the

differentiation of certain breast cancers. Dendrogram clustering analysis suggests that the

N-terminal and C-terminal domains of MT-3 differentially regulate gene expression in

MCF7 cells. Increased doming activity and increased doubling times of mutant cell lines

containing the C-terminal is suggestive of a differentiated phenotype of the cell line.

Differential regulation of GAGE antigens and E-cadherin in the presence of MT-3 could

be indicative of MT-3's role in the epithelial to mesenchymal transition of cancer cells.

CHAPTER I

INTRODUCTION

Overview

This study focused on creating a model system to study the effects that MT-3 and its unique N- and C-terminal domains have on the growth and differentiation of breast cancer. This laboratory has previously demonstrated the overexpression of MT-3 is correlated to a poor diagnostic outcome in breast cancer patients. The creation of MCF7 cell lines expressing the N-terminal, C-terminal, or both of MT-3 followed by the subsequent microarray analysis will yield insight into the role of MT-3 in the differentiation of breast cancer. Subsequent investigation into differentially regulated genes may elucidate targets for breast cancer therapy.

Breast Cancer

There are roughly 232,670 females and 2,360 males diagnosed with breast cancer every year. Approximately 40,000 females and 430 males die from breast cancer disease annually as well (Jemal et al. 2002). For women in the United States breast cancer is the leading cause of mortality from cancer. Over the course of a lifetime one in eight females will be diagnosed with breast cancer. The BRCA1 and BRCA2 genes are linked to a high susceptibility of breast cancer but only occur in five percent of breast cancer

patients (Schmid et al. 1993), while many breast cancers contain point mutations in exons

five through eight of the P53 gene indicating the occurrence may be due to xenobiotic-

induced mutations (Biggs et al. 1993). This leaves the mechanism of occurrence for the

majority of breast cancers unknown. Evidence suggests that various sources of excess

estrogen correlate to eventual breast cancer development (Henderson et al. 1982).

Obesity also increases the risk of breast cancer by 80% for every 10 kg of body weight

added post menopause (de Waard and Baanders-van Halewijn 1974). Diets high in fiber

rich foods may also reduce breast cancer risk since fiber prevents the intestinal

reabsorption of excreted estradiols (Cohen et al. 1991). Additionally macro- and

micronutrient balance appear to play a role in genomic regulation, and preliminary data

suggest that specific nutrient rich foods have a protective epigenetic effect. Identifying

the influence of environmental toxicants, hormonal exposure, nutrition, and disease on

epigenetics and changes in gene regulation may have potential for development of new

therapeutic approaches for the prevention of breast cancer (Hill and Hodsdon 2014).

There are three main types of breast cancer cases: ductal carcinoma *in situ,*

invasive ductal carcinoma, and lobular carcinoma *in situ*. Growth of breast cancer is

often dependent on the overexpression of the estrogen receptor (ER) with seven out of ten

breast cancers being categorized as ER+. Overexpression of the epidermal growth factor

receptor (HER2) occurs in 30% of breast cancer cases and is associated with an

aggressive phenotype (Ross-Innes et al. 2012). Antiestrogens, such as tamoxifen citrate,

inhibit the binding of estradiol to the ER receptor making them useful in the treatment of

ER positive breast cancers (Rockhill et al. 1998). Tamoxifen citrate negates the

stimulatory effects of estradiol, decreases circulating IGF-1 levels, and holds the cell in

the G1 phase of the cell cycle (Bernstein et al. 1990). Tamoxifen citrate therapy has been

utilized as a standalone treatment, paired with chemotherapy, or used after chemotherapy

treatment of breast cancer with long-term treatments of more than one year conferring a

survival advantage to patients using the therapy (Henderson et al. 1983).

The MCF7 cell line was isolated from a sixty nine year old Caucasian female, and

is derived from a malignant adenocarcinoma in a pleural effusion (Soule et al. 1973).

The MCF7 cell line is non-doming, ER+, lacks Her2/neu receptor overexpression, has a

karyotype of sixty-six to eighty-seven chromosomes, has an observed doubling time of

twenty-nine hours, and has no basal expression of MT-3 (Gurel et al. 2003). Since the

MCF7 cell line retains the characteristics of the mammary epithelium it is widely used for

in vitro breast cancer studies (Lacroix and Leclercq 2004). The MCF7 cell line is able to

form tumors in athymic mice with estrogen supplementation (Pratt and Pollak 1993).

Knowledge of the signal transduction and molecular biology of estrogen stemmed from

research conducted with MCF7 cells and depended on the cell lines unique properties

(Levenson and Jordan 1997).

Metallothionein

Metallothioneins are a group of intracellular proteins with a high binding affinity

for metals. They are cysteine-rich and are of low molecular weight (six to seven kDa),

and are typically a single polypeptide chain of sixty to sixty-eight amino acids.

Metallothioneins have a unique amino acid composition that consists of twenty conserved

cysteine residues and contain no aromatic amines or histidine. Metallothionein was

initially characterized as a Cd^{2+} binding protein first isolated from equine kidney cortex

in 1957 by Margoshes and Vallee (Thirumoorthy et al. 2007). Presently metallothioneins are classified into four subgroups, MT-1, MT-2, MT-3, and MT-4. In humans the MT genes are located at chromosome 16q13 and have twelve functional (MT-1A, MT-1B, MT-1E, MT-1F, MT-1G, MT1H, MT-1L, MT-1M, MT-1X, MT-2A, MT-3, and MT-4) and four nonfunctional (MT-1C, MT-1D, MT1I, and MT1J) isoforms. Both MT-1 and MT-2 isoforms are distributed in tissues throughout the human body, whereas MT-3 and respectively found in the nervous system and kidney, and stratified epithelia (Cherian, Jayasurya, Bay 2003).

Metallothioneins are physiologically important for the role they play in the homeostasis of essential metals such as zinc and copper during growth and development (Cousins 1983). They also provide protection against reactive oxygen species, alkylating agents, and act to attenuate heavy metal-induced toxicity (Cherian, Jayasurya, Bay 2003). Metal ions are bound in two distinct clusters, one near the N-terminal which binds three metal ions to nine cysteine residues, and the other near the C-terminal which binds four metal ions to eleven cysteine residues (Thirumoorthy et al. 2007) (Figure 1). Metallothioneins are therefore able to donate zinc or copper to metallo-enzymes and transcription factors. The binding affinity for metal ions to MTs is $Zn^{2+} < Cd^{2+} < Cu^{+} < Hg^{2+} < Ag^{+} = Bi^{3+}$. The Zn^{2+} ion is readily displaced by toxic metal ions enabling MTs to attenuate the toxic effects of those ions (Miles et al. 2000). Metallothioneins bind Zn^{2+} in the human body thus acting as a reservoir of the metal ion for later use. These Zn^{2+} ions play a role in various biological processes including DNA synthesis, enzymatic catalysis, gene expression, and apoptosis. Deregulation of zinc transporters occurs in breast cancer

and results in an altered level of Zn^{2+} and MTs in the plasma. The role that Zn^{2+} and MTs may play in cancer pathogenesis is still unknown (Gumulec et al. 2011).

The expression of metallothioneins is also associated with protection against DNA damage and apoptosis. Metallothioneins may function as transcriptional co-factors by donating zinc, and during cell proliferation and differentiation metallothioneins can translocate from the cytoplasm to the nucleus (Cherian, Jayasurya, Bay 2003). Increased expression of metallothioneins has been observed in human liver, lung, kidney, colon, ovary, prostrate, nasopharynx, testes, salivary gland, thyroid, bladder, and breast tumors. There is a down regulation of metallothionein expression in hepatocellular carcinoma and liver adenocarcinoma (Cherian, Jayasurya, Bay 2003).
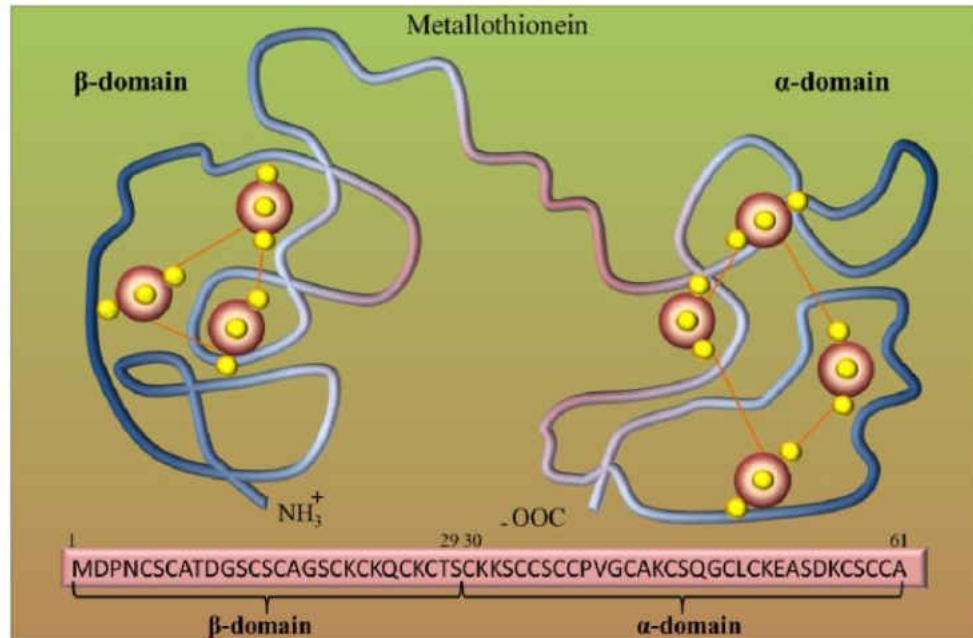
Figure 1: Diagram depicting the binding of metal ions in the α and β domain of metallothionein by thiolate clusters with a representative MT amino acid sequence. Metal ions are represented by red spheres and sulfur atoms are represented by yellow spheres. The β-domain is able to bind three metal ions, while the α-domain is able to bind four metal ions. Adapted from (Ruttkay-Nedecky et al. 2013).

Metallothionein gene expression can be induced by the presence of cytokines, metals, and hormones (Bremner 1991). Glucocorticoid, antioxidant, cyclic AMP, interferon, and TPA-responsive elements are present in the promoter region of metallothionein genes (Samson and Gedamu 1998). The presence of heavy metals increases metallothionein expression through multiple metal response elements (MREs) present in the promoter regions of all metallothionein genes (Karin et al. 1984). Transcription factors found to bind MREs and induce gene expression include the zinc activated protein, MTF-1, zinc regulation factor, and metal response element binding factor (Czupryn, Brown, Vallee 1992).

The zinc sulfur interaction in metallotioneins provides a chemical basis where the cysteine group can act as a ligand and carry out oxidoreductive reactions (Maret 2004). Cysteinyl thiolate groups scavenge free hydroxyl and superoxide radical in a quenching process that involves all twenty cysteine residues, and occurs at a reaction rate 340 fold higher than the rate for GSH (Thornalley and Vasak 1985). Under normal conditions metallotioneins are concentrated in the cytoplasm, however, after treatment of cells with hydrogen peroxide, MT-1 MT-2 are rapidly translocated to the nucleus indicating that they may play a role as a nuclear antioxidant (Takahashi, Ogra, Suzuki 2005).
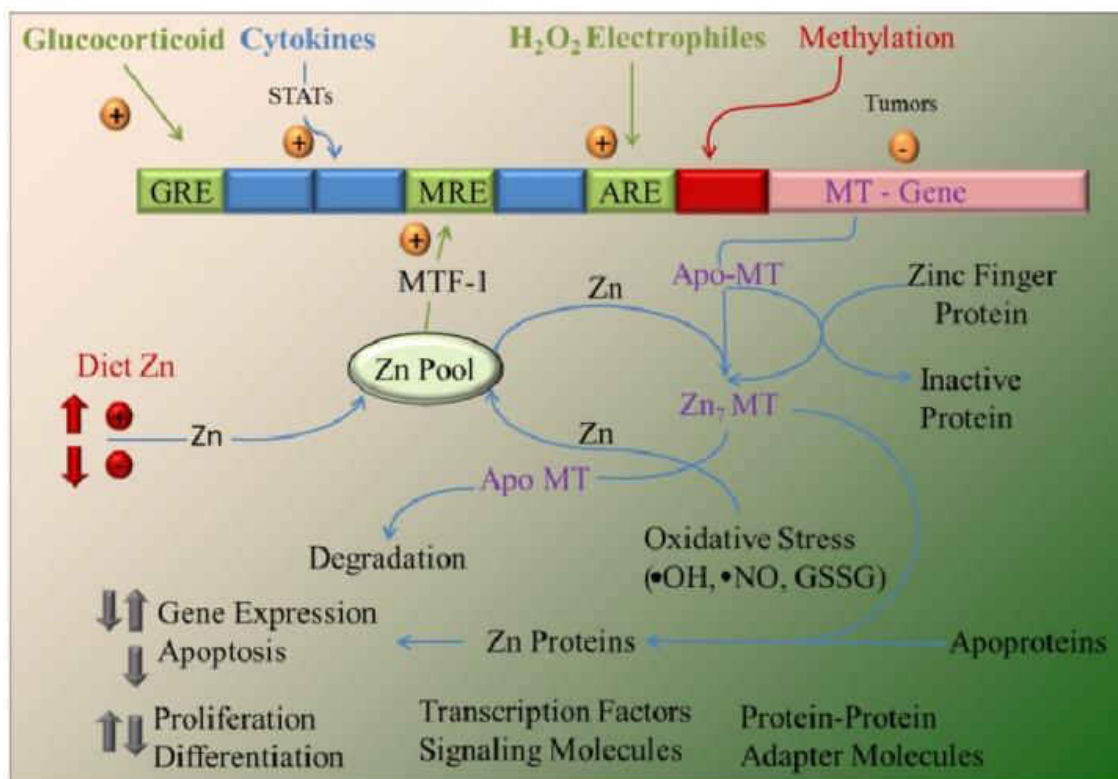
Figure 2: Metallothionein gene regulation and function. The metallothionein promoter contains several response elements that regulate transcription. These include MRE, GRE, ARE, and STAT elements. Adopted from (Ruttkay-Nedecky et al. 2013).

Metallothionein-3

This isoform was first identified as a growth inhibitory protein in a study conducted by Uchida. It was discovered that the survival rate of rat neonatal cortical neurons cultured with protein extracts from brains with Alzheimer's disease (AD) increased in comparison to those supplemented with normal brain extract (Uchida et al. 1991). The increase in neurotrophic activity and survival of the cortical neurons in the AD brain was due to the absence of this growth inhibitory protein, which decreases neurotrophic conditions under normal circumstances (Uchida et al. 1991). Further studies characterizing the molecule eventually revealed that the inhibitory molecule retained all the classic characteristics of a metallothionein, prompting it to be redesignated as MT-3 (Tsuji et al. 1992). The growth inhibitory activity is unique to MT-3 as none of the other isoforms are associated with this phenomenon (Ding, Ni, Huang 2010). Metallothionein-3 may also play an important role in lysosome function. In the absence of MT-3 there is a reduction of lysosomal enzymes, and decreased autophagic flux in astrocytes (Lee and Koh 2010).

Even though MT-3 conserves approximately 70% of the amino acid sequence found in other MT isoforms, it is structurally unique in comparison to the other isoforms. The carboxy-terminal region (C-terminal domain) contains a unique acidic hexapeptide stretch EAAEAE, while an additional threonine residue is present in the amino-terminal region (N-terminal domain). Those additional seven amino acids are not found in any of the other MT isoforms (Uchida et al. 1991). The growth inhibitory activity of MT-3 is abolished by a double mutation in the N-terminal region resulting in the conversion of the

8

conserved TCPCP sequence to either TCSCA or TCSCT. This implicates the N-terminal region of MT-3 in the growth inhibitory activity of MT-3 (Sewell et al. 1995). The discovery that MT-3 possessed this unique biological property spurred interest into researching potential biological activities of all the MT isoforms. Transgenic mice expressing MT-3 ectopically, in the same expression domain of MT-1, died of pancreatic acinar cell necrosis at 2-3 months of age (Quaife et al. 1998). Transgenic MT-3 knock out mice exhibited sensitivity to aggravated neuronal damage following a middle cerebral artery occlusion when compared to WT mice (Koumura et al. 2009). Growth inhibitory activity of MT-3 outside the neuronal system was demonstrated by stable expression of MT-3 in kidney, PC-3 prostate cancer cells, MCF7, and T-47D cell lines; however growth inhibitory activity did not occur when MT-3 was expressed in Hs578T and MDA-MB-231 cell lines (Dutta et al. 2002; Gurel et al. 2003).

The EAAEAE insert in MT-3 forms part of the backbone of the molecule and unlike MT-1/2 is not restricted by the metal-thiolate cluster enabling MT-3 to have a more dynamic loop conformation (Ding, Ni, Huang 2010). Deletion of the EAAEAE sequence leads to decreased bioactivity due to the α-cluster being able to constrict further and alter domain-domain interactions (Ding, Ni, Huang 2010).

Expression of MT-3 was initially thought to be restricted to the central nervous system, but expression of MT-3 has been detected in the normal human kidney, renal carcinoma, bladder cancer, and prostatic adenocarcinoma (Albrecht et al. 2008; Cherian, Jayasurya, Bay 2003). The overexpression of MT-3 in human breast cancer cases has been correlated to poor prognosis (Sens et al. 2001). Unlike the MT-1/2 isoforms MT-3 expression is not induced by metals; however it has been demonstrated that expression of

MT-3 mRNA can be induced transiently, under the control of metal regulatory elements, in the proximal tubule cells once they are exposed to cadmium (Garrett et al. 2002). Previous studies provide evidence that MT-3 has specific patterns of expression, induction, and regulation and that further research into the role of MT-3 in breast cancer will provide new insights into the function of this metallothionein isoform.

Metallothionein-3 and Breast Cancer

Metallothionein-3 is not expressed in normal breast epithelial cells, but is highly expressed in the majority of breast tumor samples (Sens et al. 2001). The role that MT-3 plays in the differentiation of breast cancer has yet to be fully described. The MCF7 cell line has no basal expression of MT-3, and does not form domes in cell culture. The formation of domes indicates a differentiated phenotype capable of vectorially active transport (Claude 1978). Overexpression of MT-3 in MCF7 or Hs578T cells results in growth inhibition while the overexpression of MT-1E does not result in growth inhibition (Gurel et al. 2003b). Overexpression of MT-3 in cancer cell lines also results in increased drug resistance (Dutta et al. 2002).

Excess MT-3 may produce an excess of metal-free MT (apoMT) and in so doing generate a zinc-deficient state. The creation of a zinc-deficient state may result in the dysregulation of zinc finger transcription factors (Hainaut and Milner 1993; Oren and Prives 1996; Zeng, Vallee, Kagi 1991) causing cell growth, differentiation, and programmed cell death to be affected. The zinc-deficient state may also induce a p53-null state since apoMT has the potential to sequester zinc from p53 similarly to other zinc chelators (Garrett et al. 1999). Overexpression of MT-3 in tumors may cause a zinc-

limiting cellular environment that favors tumor progression despite the slowed cellular growth (Sens et al. 2001).

The presence of cadmium in human breast cancers indicates that cadmium may play a role in progression and development of the cancer (Antila et al. 1996). Cadmium may act as an environmental estrogen by binding to and activating the ER-α receptor (Garcia-Morales et al. 1994). Zinc was unable to induce the same increase in growth that cadmium was (Garcia-Morales et al. 1994). Since MT-3 expression is induced by the presence of cadmium, studying the effect of the presence of MT-3 may yield new insights into breast cancer biology.

Metallothionein-3 and E-cadherin Expression in HK2 Cells

Fibrosis in chronic renal disease is due to toxic insult from many sources. Such sources include diabetes and hypertension, and recent evidence suggests that environmental exposure to the heavy metal nephrotoxin, cadmium, may also contribute to this process. In renal fibrosis seen in chronic renal disease, nearly one third of the resident fibroblasts derive from the proximal tubule epithelium, and the process by which this occurs is termed the epithelial-to-mesenchymal transition (EMT). To better understand EMT an *in vitro* model system has been developed that consists of the normal, immortalized human proximal tubule cell line, HK2. The HK2 cell line lacks several attributes seen in mortal cultures of human proximal tubules cells such as the lack of cell junctions, vectorial active transport, and E-cadherin expression, characteristics which are also exhibited in mesenchymal cells. Restoration of MT-3 expression in this cell line led to an establishment of cellular junctions, vectorial active transport, and a

cadherin expression profile that is consistent with an epithelial phenotype (Bathula et al.

2008)(Figure 3). Expression of E-cadherin is essential for this transition due to the role

of E-cadherin in the establishment of adherens junctions, which is required for vectorial

active transport. Current studies suggest that the EMT process itself may be controlled

by MT-3 mediated transcriptional regulation of the E-cadherin gene. E-box elements in

the E-cadherin promoter allow for repression of E-cadherin (Batlle et al. 2000).
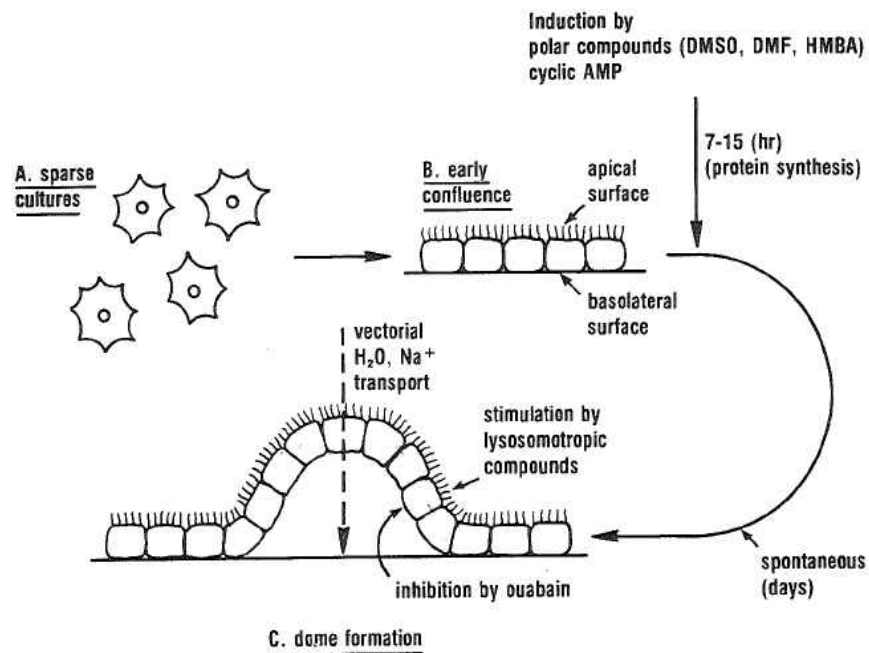
Figure 3: Dome formation by vectorial active transport. Dome formation occurs

when a monolayer of epithelial cells differentiates to possess apical and basolateral

surfaces (Lever Julia 1985). E-cadherin expression is required, and loss of transport

occurs during renal fibrosis. Figure adapted from (Lever Julia 1985).

GAGE Antigens

Cancer/testis (CT) antigens are a group of proteins normally expressed in human germline cells and are present in various tumor types. Currently there are eighty nine CT antigens all of which are encoded on the X chromosome (Gjerstorff and Ditzel 2008). The GAGE antigens are a family of CT antigens consisting of at least sixteen different genes, which are further divided into three groups based on their unique properties and are located on chromosome X at p11.23 (De Backer et al. 1999). GAGE-1 contains a C-terminal sequence not found in any of the other seven members. The remaining members have amino acid sequences that are 98% identical, but can be divided into two separate groups. GAGE-2 and GAGE-8 do not contain a tyrosine residue that may be phosphorylated (Y9), while GAGE-3-7 and GAGE-1 do not possess the same tyrosine residue (Salomon et al. 2003). The promoters of the GAGE antigen family have no TATA box, and have only one or two different base pairs in the first fourteen hundred base pairs (Gjerstorff and Ditzel 2008). The lack of a TATA box site for initiation allows transcription to start from several different sites leading to transcripts of varying lengths (Cilensek et al. 2002).

The exact biological function of the GAGE antigens has yet to be fully elucidated, but recent evidence suggests that they may direct cell proliferation, differentiation, and the survival of germ line cells (Simpson et al. 2005). Antiapoptotic properties have also been attributed to GAGE antigens (Cilensek et al. 2002). Expression of the GAGE antigens normally occurs in a subset of oocytes in the adult ovary (Gjerstorff et al. 2006), adult male germ cells, and for a few weeks in fetal Leydig and Sertoli cells during the third trimester (Gjerstorff et al. 2007). GAGE gene transcripts are present in numerous

types of cancers including 26% of breast cancers (Gjerstorff et al. 2006).

Immunohistochemical analysis reveals a lower level frequency of GAGE antigen

presence and a high degree of tumor heterogeneity (Kobayashi et al. 2000). The

expression of GAGE antigens in stomach cancer, neuroblastoma, and esophageal

carcinoma has been correlated with a poor prognosis and an aggressive tumor type

(Cheung, Chi, Cheung 2000; Kong et al. 2004; Zambon et al. 2001). Since most normal

tissues do not express GAGE antigens and areas of normal expression are immune-

privileged sites this makes them potentially useful targets as diagnostic and prognostic

indicators, and as potential targets for immunotherapy treatment (Gjerstorff and Ditzel

2008).

Matrix Metalloproteinases

Matrix metalloproteinases (MMPs) are a family of zinc dependent extracellular

proteases that can completely remodel the extracellular matrix (ECM) allowing MMPs to

function in a variety of biologic processes (Yadav et al. 2014). These biological

processes include: cytokine modulation, angiogenesis, growth factor bioavailability, cell

migration, cell proliferation, receptor shedding, invasion, metastasis, and apoptosis (Roy

and Walsh 2014). The epithelial to mesenchyme transition (EMT) is a multistage process

in which alteration of the microenvironment and cell differentiation is required for

metastasis to occur. During carcinogenesis MMPs act as mediators of alterations

observed in the microenvironment during both early and late stages of disease

progression (Yadav et al. 2014). In breast cancer MMPs are over expressed prior to

EMT, but treatment of cells with centchroman reversed EMT by downregulating the HER2/ERK1/2/MMP-9 pathway (Khan et al. 2015).

Leucine-Rich Repeat-Containing Proteins

Leucine rich repeat containing (LRRC) proteins are a family of proteins known to be involved in protein-protein interactions and contain multiple LRR motifs of twenty to thirty amino acids. The protein LRRC49 is a member of this family of proteins and has been shown to have elevated expression levels in ER+ breast cancers compared to ER- breast cancers, however its role in the differentiation of breast cancer remains unknown (De Souza Santos et al. 2008).

Neural Tissue-specific Epidermal Growth Factor-like Repeat Domain-containing Protein

Neural tissue-specific epidermal growth factor-like repeat domain containing protein two (NELL2) was first discovered as a mammalian homolog to the chicken NEL protein. It has been found to be expressed in neurons. NELL2 may play a role in neuronal development, postnatal neural activity, and in cancer cell survival. Overexpression of NELL2 occurs in Burkitt's lymphoma and in neuroblastomas (Maeda et al. 2001). Recent studies have revealed that the expression of NELL2 is regulated by the oncogene E2F1 (Kim et al. 2013). The E2F1 oncogene is a key regulator of cell proliferation. Overexpression of NELL2 also increases the invasive activity of MCF7 and MDA-MB-231 cells (Kim et al. 2013).

Bifunctional 3'-phosphoadenosine 5'-phosphosulfate synthetase 2

Bifunctional 3'-phosphoadenosine 5'-phosphosulfate synthetase 2 (PAPSS2) is an enzyme that acts as a sulfur donor and catalyzes the transfer of sulfur to other molecules in a process known as sulfation. Estrogen is metabolized and inactivated in target tissues via sulfation effectively inactivating the molecule to elicit growth. It has been demonstrated that overexpression of PAPSS2 in MCF7 slows cellular proliferation both *in vivo* and *in vitro* arresting cell cycle progression and inducing apoptosis (Xu et al. 2012).

Glycogen Phosphorylase

The metabolic enzyme glycogen phosporylase (PYGL) plays a role in the metabolic reprogramming of cancer cells. In the hypoxic environment of a growing tumor glycogen metabolism is upregulated (Favaro et al. 2012). The degradation of glycogen by PYGL is necessary for the function of the pentose phosphate pathway and cells without sufficient levels of PYGL undergo senescence (Favaro et al. 2012). Inhibition of PYGL and the subsequent metabolic alterations induces senescence in glioblastomas making it a potential therapeutic target (Abbadi et al. 2014).

Voltage-Gated Sodium Channels

Voltage gated sodium channels (VGSCs) are normally expressed in cells of the nervous system, and are responsible for the rising phase of action potentials (Pablo and Pitt 2014). Expression of VGSCs also occurs in various metastatic cells and in specific cancer cell lines including the prostate (Shan et al. 2014). Expression of the α subunits of the sodium channels Nav1.6 and Nav1.7 were found to be six to twenty-seven times

higher in PC-3 and LNCaP cells than in cells of benign prostatic hyperplasia (Shan et al. 2014). The overexpression of these subunits could serve as both a therapeutic target and prognostic biomarker.

Statement of Purpose

This study is designed to further elucidate the role of MT-3 in the regulation of cell differentiation in breast cancer. The study aims to elucidate the role that the unique N- and C-terminal domains of MT-3 may play in the differential expression of genes involved in the progression of breast cancer. MT-3 has been shown to be overexpressed in poor prognosis breast cancers (Sens, et al 2001), and has been shown to inhibit the growth of breast cancer and prostate cancer cell lines stably expressing MT-3 (Gurel, et al 2003). When compared to other MT isoforms MT-3 contains an additional Thr in the N-terminal region and an acidic hexapeptide sequence EAEAAE in the C-terminal domain not found in other members of the MT gene family. It was determined that the non-doming MCF7 cell line would be used to study MT-3 and its role in breast cancer since MCF7 cells have no basal expression of MT-3.

In order to characterize the function of the N- and C-terminal domains of MT-3 in the MCF7 breast cancer cell line six different constructs of MTs will be prepared as follows: wild type (WT) MT-3, MT-3 N-terminal point mutation (MT-3 P7T P9T), MT-3 C-terminal deletion (MT-3 E55_E60del), WT MT-1E, and MT-1E insert mutation to contain the N -terminal of MT-3 (MT-1E N4_C5insTCPCP), or the C-terminal (MT-1E G52_A53insEAAEAE), or both the N- and the C-terminal of MT-3 (MT-1E N4_C5insTCPCP and G52_A53insEAAEAE). Each of these constructs will be

transfected into MCF7 cells and three cell lines with the highest expression levels as determined by real time PCR and dot blot determination of protein levels will be utilized for observations. Cell cultures will be observed for the formation of domes, doubling times will be determined using the MTT method, and the transepithelial resistance (TER) of each cell line will be measured to determine if vectorially active transport is occurring.

Microarray analysis of the MCF7 mutants will also be performed to determine alterations in global gene expression. The bioinformatics core at the University of North Dakota School of Medicine and Health Sciences will analyze the microarray results for differentially expressed genes in the MCF7 mutant cell lines. Overlap hierarchal clustering will be utilized to demonstrate and visualize the expression relationship between the N- and C-terminal mutants. Differentially expressed genes based on microarray analysis will be confirmed by real time PCR. This study may provide evidence regarding MT-3's role in the differentiation of breast cancer, and elucidate the role the N- and C-terminal domains of MT-3 play in differentiation.

CHAPTER II

MATERIALS AND METHODS

Reagents

TRI Reagent and bromo-chloropropane (BCP) Phase separation reagent were purchased from Molecular Research Center, Inc. (Cincinnati, OH) 1.5 M Tris-HCl, ammonium persulfate, TEMED, Laemmli sample buffer, 0.5 M Tris-HCl, SYBR green PCR kits, cDNA synthesis kits, and pre-cast PAGE-gels were purchased from BIO-RAD. (Hercules, CA) Albumin standards and BCA protein assay reagents were purchased from Pierce (Rockford, IL). Glutaraldehyde solution, isopropanol, methanol, ethanol, DMEM nutrient, and F12 nutrient were purchased from Sigma-Aldrich (St. Louis, MO). Fetal calf serum, penicillin-streptomycin 10,000 U/mL, and trypsin–ethylenediaminetetraacetic acid (0.05%, 0.02%) were purchased from Gibco (Life Technologies, NY). Hydrophilic Polytetrafluoroethylene trans-well inserts designed for 6-well cell culture dishes were obtained from Millipore (EMD Millipore, MA). For the microarray analysis the HumanHT-12 v4 Expression BeadChip (Illumina, CA) was selected.

METHODS

Cell Culture

The MCF7, and Hs578-T cells were obtained from American Type Culture Collection (Rockville, MD), and grown in Dulbeco's Modified Eagles Medium (DMEM) (which contains 1000 mg/L glucose and L-glutamine, supplemented with 100 units/mL penicillin, 100 µg/mL streptomycin, 0.25 amphotericin B, 0.205 µg/mL sodium deoxycholate, and 3.7 g/L sodium bicarbonate) supplemented with 5% (v/v) fetal calf serum, 5 mg/ml glucose and routinely passaged at a 1:4 ratio upon attaining confluence. HK2 and HK2-MT3 cells were cultured using a growth formulation consisting of a 1:1 mixture of DMEM and Ham's F-12 (which contains L-glutamine 0.146 g/L, supplemented with 100 units/mL penicillin, 100 µg/mL streptomycin, 0.25 µg/mL amphotericin B, 0.205 µg/mL sodium deoxycholate, and 3.7 g/L sodium bicarbonate) growth medium supplemented with selenium (5 ng/ml), insulin (5 µg/ml), transferrin (5 µg/ml), hydrocortisone (36 ng/ml), triiodothyronine (4 pg/ml), and epidermal growth factor (10 ng/ml). MCF7 cells and Hs578-T cells were fed every 3 days. HK2 and HK2-MT3 cells were fed fresh growth medium every 3 days and 2 days respectively. The cells were kept in various tissue culture vessels at a constant temperature of 37° C in a 5% CO_2 : 95% atmosphere. Medium was always replaced with fresh medium 24 h prior to subculturing. Upon obtaining confluency, cells were subcultured in the following manner: culture medium was aspirated and the cells were rinsed twice with sterile PBS (37° C) then trypsin–ethylenediaminetetraacetic acid (0.05%, 0.02%) (Life Technologies, NY) was added to the vessel. The cells were monitored until disassociation from the bottom of the culture vessel occurred. The cell suspension was then transferred to a

conical tube containing fetal calf serum (Gibco, Mexico) using additional PBS to suspend and transfer the cells. A cell pellet was obtained by a five min centrifugation at 2,000 rpm followed by the removal of the supernatant. Cell pellets were resuspended in an appropriate volume of medium, and then seeded in the desired culture vessel. Culture vessels were then placed in the incubator and cells were evenly distributed by gentle shaking in horizontal and vertical directions.

Electroporation

Transfection of HK2 and HK2-MT3 cells was performed with Amaxa Cell Line Nucleofector Kit V (Amaxa, NJ) according to the manufacturer's protocol. Cells were suspended in Nucleofector Solution to a final concentration of 3×10^6 cells/100 μl. The cells were transfected using 2 μg of the Luciferase reporter construct, and 0.2 μg of the Renilla reporter construct. (Promega, WI) In amaxa-certified cuvettes, the cells were nucleofected using the program T-020. The nucleofected cells were transferred to 2000 μL of prewarmed medium in 6-well plates after adding 500 μL prewarmed medium directly to the cuvette, and incubated for 36 h.

E-Cadherin Promoter Constructs

Vector Construction

Wild Type Promoter Region of E-cadherin

CCCATAACCCACCTAGACCCTAGCAACTCCAGGCTAGAGGGTCACCGCGTCT
ATGCGAGGCCGGGTGGGCGGGCCGTCAGCTCCGCCCTGGGGAGGGGTCCGC
GCTGCTGATTGGCTGTGGCCGG<u>CAGGTG</u>AACCCTCAGCCAATCAGCGGTACG

GGGGGCGGTGCCTCCGGGGCT<u>CACCTG</u>GCTGCAGCCACGCACCCCCTCTC<u>A</u>G

TGGCGTCGGAACTGCAAAG<u>CACCTG</u>

E-cadherin Promoter with Mutated E-boxes

CCCATAACCCACCTAGACCCTAGCAACTCCAGGCTAGAGGGTCACCGCGTCT

ATGCGAGGCCGGGTGGGCGGGCCGTCAGCTCCGCCCTGGGGAGGGGTCCGC

GCTGCTGATTGGCTGTGGCCGG**AACCTA**AACCCTCAGCCAATCAGCGGTACG

GGGGGCGGTGCCTCCGGGGCT**AACCTA**GCTGCAGCCACGCACCCCCTCTC<u>A</u>G

TGGCGTCGGAACTGCAAAG**AACCTA**

Mutated E-box regions are in bold. The WT E-boxes and mutated E-box regions are underlined and the transcription start site is a single underline A. The above sequences were ligated into the multiple cloning region of the pGL4.10[*luc2*] vector (Promega, WI) by GenScript (Piscataway, NJ). The desired promoter sequence, length, and mutation of the E-boxes are based on research previously conducted by Batlle (Batlle et al. 2000b). Sequence design for ligation was done utilizing Vector NTI® computer software (Life Technologies, NY).

Luciferase Assay

The HK2 and HK2-MT-3 cell lines were transfected with the promoter reporter constructs previously described. Transfected cells were rinsed with prewarmed PBS once, before adding 500 µL of Promega's supplied lysis buffer PLB. Cells were gently rocked for fifteen minutes to allow for complete lysis. A total of 20 µL of cell lysate was added to 100 µL of Luciferase assay reagent, and the intensity of luminescence was measured using the Biotek FLx800 plate reader. The Luciferase reaction was then

quenched using 100 µL of Promega's Stop and Glo buffer, and then the luminescence of the Renilla was measured. Lysates were measured four separate times per electroporation reaction. The use of the Renilla reporter under the thymidine kinase promoter was used to normalize for transfection efficiency.

Stable Transfection of MCF7 Cells

The WT MT-3, WT MT-1E, MT-3ΔNT (MT-3 P7T P9T), MT-3ΔCT (MT-3 E55_E60del), and NT-1E (MT-1E N4_C5insTCPCP), CT-1E (MT-1E G52_A53insEAAEAE), and CT-NT-1E (MT-1E N4_C5insTCPCP and G52_A53insEAAEAE) were blunt end ligated into the 6.2/V5 Destination vector (Invitrogen, NY) were linearized using BspHI (New England Biolabs, MA) prior to transfection using Effectene reagent (Qiagen, CA) (Figure 4). Sequence design for ligation was done utilizing Vector NTI® computer software (Life Technologies, NY). Generation of the mutant sequences and ligation the genes was conducted by GenScript (Piscataway, NJ) using the WT MT-3 gene sequence. Plasmids were transformed using One Shot® TOP10/P3 *E. coli* cells (Life Technologies, NY) and purified using a Qiagen midi prep kit (Qiagen, CA).

Transfected cells were allowed to reach confluency in one well of a 6-well plate and then subcultured at a 1:10 ratio into a 6-well plate. Transfected cells were propagated using media containing 10 µg/mL blasticidin (Invitrogen, CA) and observed for the formation of small isolated colonies. Twenty four colonies were selected for each construct by using cloning rings that held 200 µL in volume (Sigma Aldrich, MO) and were always exposed to media containing 10 µg/mL blasticidin (Invitrogen, CA).

Selected colonies were subcultured into one well of a 24-well plate. Upon attaining confluency transfected cells were subcultured into one well of a 12-well plate for a 1:2 split ratio. Colonies of transfected cells were subcultured a final time into a 6-well plate prior to a portion of the cells being harvested for mRNA isolation. Cell lines expressing $1\text{x}10^5$ copies of the mRNA per 10 ng RNA were selected using qRT-PCR. Protein expression for each cell line was determined using the dot blot method, and the three cell lines expressing the highest amount of protein were selected for downstream applications.
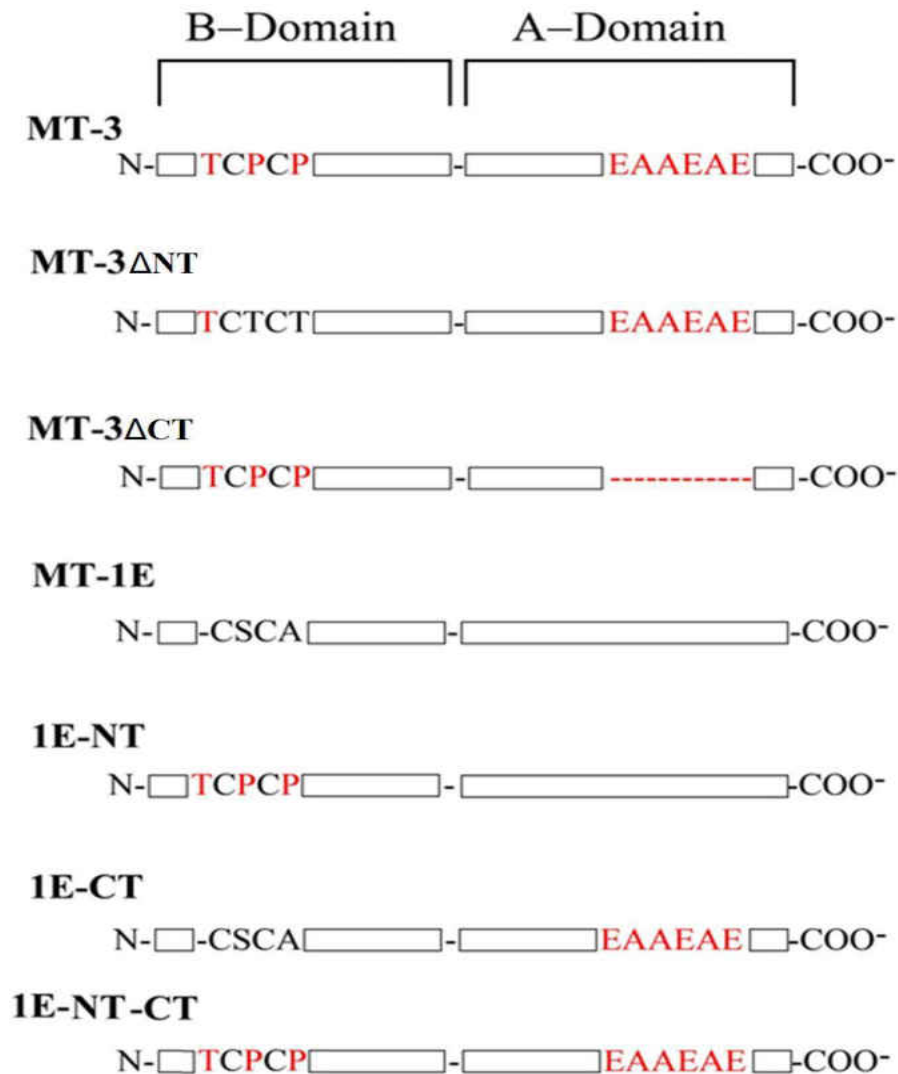
Figure 4: **Visual representation of the gene constructs generated to further examine the role of the unique N- and C-terminal domains of MT-3.** Constructs of MTs were prepared which were as follows: wild type (WT) MT-3, MT-3 N-terminal mutation (MT-3 P7T P9T), MT-3 C-terminal deletion (MT-3 E55_E60del), WT MT-1E, and MT-1E mutated to contain the N-terminal of MT-3 (MT-1E N4_C5insTCPCP), or the C-terminal (MT-1E G52_A53insEAAEAE), or both the N- and the C-terminal of MT-3 (MT-1E N4_C5insTCPCP and G52_A53insEAAEAE).

Transfection of MCF7 Cells Using Qiagen Effectene

Cells were split 24 h prior to transfection and were allowed to achieve 40-60% confluency. A 1:10 ratio of DNA to Effectene was utilized for the procedure. Linearized DNA was diluted to .1 µg/µL in Tris-EDTA, and a total of 1 µg DNA was used per transfection. Qiagen supplied all needed reagents the formulation of which is proprietary. Diluted DNA was combined with 90 µL of buffer EC and 4 µL of Enhancer. The combination was mixed, spun down briefly, and incubated at room temperature for 2-5 minutes. A total of 10 µL Effectene was added to the mixture, incubated for 5-10 min at room temperature, and then combined with 400 µL media prior to being added to the cells. Before the DNA and Effectene complex was added to the cells they were rinsed once with PBS and had fresh media added to the culture vessel.

Doming Observations for MCF7 Cell Lines

MCF7 parent and MCF7 mutant cell lines were seeded at a 1:3 ratio in triplicate into T-25 flasks without vented caps. Cells were all fed on a standard schedule and flasks were observed for domes once the culture obtained confluency. Dome formation observation began 6 days post seeding. A dome is considered formed when a group of several cells appears out of focus in relation to the monolayer, and when some portion of the dome is in focus the rest of the monolayer will appear out of focus. A field of view using a 10x objective has a surface area of 1,180,370.75 µm^2. Flasks were scanned and when doming was observed that field of view and all the domes in it were counted. A dome was only allowed to be counted once in one field of view. Doming cultures had twenty-one field of views observed per T-25 culture flask.

Measurement of Transepithelial Resistance

MCF7 parent and MCF7 mutant cell lines were seeded at a 1:2 ratio in triplicate onto 30-mm-diameter cellulose ester membrane inserts (Millipore, MA) placed in six-well trays. Beginning on the third day post-seeding, TER was measured every day with the EVOM Epithelial Voltohmmeter with a STX2 electrode set according to the manufacturer's instructions (World Precision Instruments, FL). This instrument measures the resistance to an alternating current flow through the filter containing the monolayer of cells. The resistance of the bare filter containing medium was subtracted from that obtained from filters containing cell monolayers. Two sets of four readings were taken at four different locations on each filter.

Determination of Doubling Times

Forty microliters of 5 mg/mL 3-(4,5-Dimethylthiazol-2-yl)-2,5 diphenyltetrazolium bromide (MTT) (Sigma Aldrich, MO) was added to the media of cells plated at a 1:100 ratio. After 3.5 h the cells were washed once with PBS, and the formazan crystals were solubilized in acidic propanol. Absorption at 570 nm was determined. Increases of absorption during the logarithmic growth phase were used to calculate doubling times.

Dot Blot and Protein Extraction Method Specific for Dot Blot

Determination of MT-3 protein content per microgram of total protein was accomplished by immunoblotting. Cells were rinsed twice with PBS, and harvested in a buffer containing 10 mM Tris pH 7.4 and 75 mM NaCl. Lysis of the cells was accomplished by freezing the cells for 30 seconds in liquid nitrogen followed by rapidly

thawing the cells in 37°C water. The freeze thaw process was repeated three times.

Samples were then centrifuged at 15,000xg for 15 minutes at 4°C the supernatant was

collected for further use. Protease inhibitors and a final concentration of 1 mM DTT was

added to each sample. A total of 2 µg of protein lysate in PBS and 1.5% glutaraldehyde

was transferred to the dot-blot apparatus. The protein lysate was transferred onto a

PVDF membrane by gravity flow. Samples were rinsed twice with PBS after having

entered the membrane. The membrane was then stained for MT-3 using the following

dot blotting protocol: the membrane was blocked using 1% BSA in PBS, following

which the membrane was incubated with the primary MT-3 antibody at a 1:100 dilution

in 1% BSA in PBS. After incubation with the primary antibody the membrane was

washed a couple of times and then incubated with the secondary anti-mouse alkaline

phosphatase-conjugated secondary antibody (Promega, WI) at a 1:500 dilution in .4%

BSA in PBS. The antigen-antibody complexes were visualized using the alkaline

phosphatase KI III (Vectore, CA). The membrane was washed three times for 15 minutes

in PBS between every step.

Cell Culture Harvest

Confluent cell cultures were harvested in the following manner: cell culture

vessels were rinsed twice with 10 mL PBS, 1.5 mL of PBS was added and the cells were

mechanically scraped from the vessel, the suspension was then added to a 1.5 mL

microfuge tube and pelleted at 2,000 rpm for 5 min at 4°C, the supernatant was aspirated

and the remaining pellet was stored at -80°C for later use.

Preparation of RNA for Microarray Analysis

Qiagen RNeasy Mini Kit (Qiagen, CA) was used to prepare RNA samples for mincroarray analysis. Media was aspirated off of confluent T-75 flasks (Corning, NY) and 3 mL of lysis buffer RLT containing 10 µL of 14.3M betamercaptoethanol per mL was added. The QiaShredder column was used to homogenize 700 µL of the lysates. An equal volume of 70% ethanol was added to the homogenized lysate, and 700 µL was added to the RNeasy mini column. The column was centrifuged at 10,000 x g for 15 seconds after which the eluate was discarded. A total of 700 µL buffer RW1 was added to column, centrifuged for 15 seconds at 10,000 x g, and the eluate was discarded. The RNeasy column was transferred to a new collection tube and the following step was done twice: 500 µL buffer RPE was added, centrifuged for 15 seconds at 10,000 x g, and the eluate was discarded. To remove all traces of remaining reagents the column was centrifuged for 1 minute at 10,000 x g with nothing added. Elution of the RNA was accomplished by adding 50 µL of RNase free water and allowing the column to equilibrate at room temperature prior to centrifugation for 1 minute at 10,000 x g.

RNA Isolation Using TRI Reagent

RNA isolation for purposes other than microarray analysis was performed using TRI reagent (Molecular Research Center Inc., OH). Following the removal of the media an appropriate volume of TRI reagent was added to the cells. Cells were incubated at room temperature for 10 minutes with gentle rocking to ensure complete lysis. The cell lysates was then pipetted repeatedly to shear the DNA prior to its transfer to an RNase free microfuge tube. A total of 100 µL BCP was added per 1 mL of TRI reagent and the samples were vortexed for a minimum of 30 seconds to ensure complete mixing. Samples were incubated at room temperature for a minimum of 5 minutes prior to being

centrifuged at 12,000 x g for 15 minutes at 4°C. The upper aqueous phase was transferred to a new tube and 500 µL of isopropanol was added. Precipitated RNA was pelleted by centrifugation at 12,000 x g at 4°C. Supernatant was removed and the RNA was washed twice with 75% ethanol followed by a centrifugation step at 7,500 x g for 5 minutes at 4°C. The RNA pellet was air dried for 2 minutes and resuspended in 30 µL of RNase free water.

Determination of DNA and RNA Concentrations

The concentration of DNA- or RNA-containing samples was determined using a Nano Drop (Thermo Scientific, TN) spectrophotometer and supplied computer software. Extinction coefficients were selected depending on if the sample was DNA or RNA. The software determined the concentration of the nucleic acid based on the absorbance at 260 nm of a 1 µL sample loaded onto the pedestal. The A260/280 ratio was also examined to determine the quality of the sample.

Determination of Protein Concentration of Cell Lysates

The protein concentration of sample lysates was determined using Bradford reagent (Bio-Rad, CA) or using the BCA assay (Pierce, IL). To make the working solution 1 part BCA reagent B was combined with 50 parts BCA reagent A, 200 µL of the working reagent was combined with 5 µL of the protein sample and 20 µL of distilled water, and incubated at 37°C for 30 min. A 1x working solution was made from 4.5x Bradford reagent and 180 µL of working reagent was combined with 15 µL distilled water and 5 µL of the protein sample. Bovine serum albumin standards at concentrations

of 0, 0.1, 0.2, 0.4, 0.6, 1.2, .1.6, and 2 µg/µL were used to make the standard curve.

Absorbance was measured at 570nm on a BioTek ELx800 (BioTek, VT).

cDNA Synthesis

Conversion of RNA to cDNA was accomplished using the iScript cDNA

Synthesis Kit (Bio-Rad, CA). Per 20 µL reaction 5 µL of 20 ng/µL RNA was mixed with

4 µL 5x iScript reaction mix, 1 µL iScript reverse transcriptase, and 10 µL nuclease free

water. The reaction was incubated using a thermocycler for 5 min at 25°C, 30 min 42°C

and 5 min at 85°C followed by storage at -20°C.

Real-time PCR Analysis Protocol for Bio-Rad Assays

Gene expression was assessed with real time RT-PCR utilizing gene-specific

primers (Bio-Rad, CA). Real-time PCR was performed utilizing the SYBR Green kit

(Bio-Rad, CA) with 2 µl of cDNA, 1 µL primers in a total volume of 20 µl in CFX real-

time detection system (Bio-Rad, CA). Cycling conditions were 94 ºC denaturation, 60ºC

annealing, and 72 ºC extension. Amplification was monitored by SYBR Green

fluorescence and compared with that of a standard curve consisting of serial dilutions of

the control cDNA (Blank Vector MCF7 cells). Gene expression is expressed as fold

change compared to the control.

Microarray Analysis

RNA isolated from each MCF7 mutant cell line using RNeasy Mini Kit (Qiagen,

CA) was sent to the University of Minnesota Genomics Center for microarray

hybridization. HumanHT-12 v4 Expression BeadChip (Illumina, CA) was utilized to

determine genome wide gene expression levels. The Bioinformatics core facility at the University of North Dakota School of Health and Medicine Sciences analyzed the resulting data for differentially expressed genes. Hierarchical clustering and principal components analysis were used to assess the similarity and variation across isolates. The fold change of each probe in each array from a transformed cell line was calculated over its average expression level in the parental MCF7 and MCF7 Blank Vector cell line. In order to test whether transformed isolates have a nonrandom set of overlapping probes, we derived a probability function for the random number of overlapping probes, and used simulation test to find the statistical significance of the observed number of overlapping probes. Differentially expressed probe sets (DEGs) were identified using empirical Bayes method (Smyth 2004) and the p-values were adjusted using false discovery rate (Strimmer 2008). The analyses were carried out using R programming language and SAS JMPH software.

<center>Transformation</center>

Plasmids received from Genscript (Piscataway, NJ) were transformed and propagated using One Shot® TOP10/P3 *E. coli* cells (Life Technologies, NY) as follows. An aliquot of *E. coli* cells were thawed on ice prior to adding 1 µL of 1µg/µL plasmid DNA in TE at pH 8.0. Cells were incubated on ice for thirty minutes and heat shocked in a water bath at 42°C for thirty seconds. Cells were placed back on ice for two minutes, prior to the addition of 250 µL room temperature S.O.C. medium. Tubes were capped and incubated with shaking at 37°C for sixty minutes. Each transformation was plated onto LB agar plates containing 100 µg/mL ampicillin and incubated at 37°C for no less

than 12 hours. Individual colonies were selected for propagation in LB media prior to plasmid isolation.

Plasmid Isolation

The Qiagen Midi Prep Kit (Qiagen, CA) was utilized to isolate plasmid DNA for downstream applications. An individual transformed colony was incubated in sterile LB media containing 10 g tryptone, 5 g yeast extract, 10 g NaCl, and 0.1 g ampicillin per liter at 37°C for 8-12 hours while shaking at 300 rpm. Cells were pelleted by centrifugation at 6000 x g for 15 minutes at 4°C, and resuspended in buffer P1 containing RNase A. Buffer P2 was added, mixed by inversion, and incubated at room temperature for five minutes. Buffer P3 was chilled to 4°C, added, mixed by inversion, and incubated on ice for five minutes. A QIAGEN-tip was equilibrated with buffer QBT prior to having the plasmid mixture applied. The QIAGEN-tip was washed twice with buffer QC, and the DNA was eluted using buffer QF. Precipitation of the DNA was accomplished by adding isopropanol, and centrifuging at 15,000 x g for thirty minutes at 4°C. The DNA pellet was washed using 70% ethanol and centrifuged at 15,000 x g for 10 minutes at 4°C. Supernatant was aspirated and the pellet was air dried for 10 minutes prior to being dissolved in TE buffer and pH 8.0.

CHAPTER III

RESULTS

Metallothionein-3 Mediated Control of E-cadherin Expression Through E-box
Promoter Elements

Previous research has indicated that E-cadherin expression is down-regulated by

the binding of the transcription factors slug and snail to promoter elements called E-

boxes (Batlle et al. 2000). Expression of MT-3 in HK2 cells restores vectorial active

transport and is accompanied by an increase in the expression of E-cadherin (Bathula et

al. 2008). The relationship between the expression of MT-3 and E-cadherin was

examined using a luciferase construct containing 205 base pairs upstream of the E-

cadherin gene start site and twenty-seven base pairs past and including the start site. This

region contains three E-box elements capable of interacting with the transcription factors

slug and snail. Mutation of the E-boxes prevents transcriptional repression by slug or

snail (Batlle et al. 2000). A construct with all three E-boxes mutated to prevent binding

and a WT version were both transfected into WT HK2 cells or HK2 cells stably

expressing MT-3 (HK2-MT-3). Thirty-six hours post-transfection, cells were assayed to

determine the relative activity of each promoter based on the amount of Luciferase

produced, and normalized for transfection efficiency by measuring the luminescence of

Renilla expressed using the thymidine kinase promoter.

The presence of MT-3 significantly increased E-cadherin expression levels in the case of the WT E-cadherin promoter construct and the mutated E-boxes promoter construct (Figure 5). Normalized luminescence was 66.13 +/- 2.53, 100.37 +/- 35.16, 135.87 +/- 42.63, and 214.7 +/- 55.03 for the WT promoter, WT promoter with MT-3, Mutated E-box promoter, and Mutated E-box promoter with MT-3 respectively. Data indicates a 47.65% increase in expression was observed in HK2 cells expressing MT-3 versus WT HK2 cells when transfected with the WT E-cadherin promoter construct, while the mutated E-box promoter construct had an 81.71% increase in expression over the WT construct in WT HK2 cells, and a 116.32% increase in expression in HK2 MT-3 cells. In HK2 cells a statistically significant increase in expression occurred when the WT E-cadherin promoter is compared to the E-cadherin promoter with mutated E-boxes (Figure S1). A statistically significant increase also occurs when comparing the expression increase of HK2 to HK2-MT-3 cells transfected with the WT E-cadherin promoter (Figure 5). Additionally, a statistically significant increase in expression occurs in the HK2-MT-3 cell line when comparing the WT E-cadherin promoter to the E-cadherin promoter containing mutated E-boxes (Figure S2).

In HK2 cells mutation of the E-boxes in the E-cadherin promoter leads to a significant increase in E-cadherin expression (Figure S1). The presence of MT-3 increases E-cadherin expression significantly for the WT E-cadherin promoter and the mutated E-boxes promoter (Figure S2). Data suggest that E-cadherin expression is modulated by the presence of MT-3 regardless of the status of the E-box elements.

Relative Expression of E-cadherin in HK2 Compared to HK2-MT3 Cells For Both Wild Type and Mutant E-box constructs

Legend:
- E-cad WT HK2
- E-cad WT HK2-MT3
- E-cad Mut E-boxes HK2
- E-cad Mut E-boxes HK2-MT3

Y axis: Ratio Luc/Ren Expression
X axis: Constructs
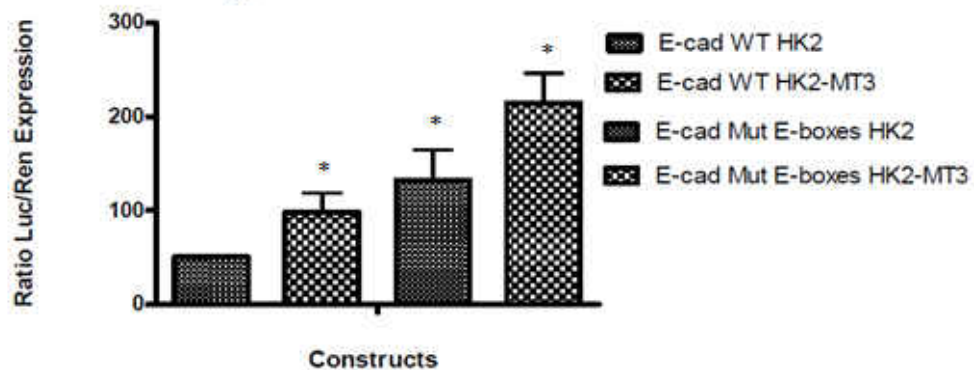
Figure 5: Comparison of both WT and Mutant E-box E-cadherin promoter constructs in both HK2 and HK2-MT-3 cell lines. Both constructs were transfected into HK2 and HK2-MT-3 cell lines and are represented on the X axis. Data are expressed as a ratio of the Luciferase signal to the Renilla signal on the Y axis. Error bars represent the standard error of the mean (SEM). Statistical significance indicated by * P-value less than 0.05 as determined using the one-way ANOVA as the test where N=3 biological replicates. Each condition is statistically significantly different in comparison to all other conditions. The HK2 cell line transfected with the WT E-cadherin promoter is utilized as the official control.

Doming Characteristics of MCF7 Cells Expressing Both or Either of the N- and C-
Terminal Domains of MT-3

Earlier work in our laboratory indicated that the restoration of MT-3 expression in
the HK2 cell line led to an establishment of cellular junctions, vectorial active transport,
and a cadherin expression profile that is consistent with an epithelial phenotype (Bathula
et al. 2008) (Figure 3). One goal of this study was to observe if either the N- or C-
terminal domain of MT-3 is responsible for the doming phenotype and if one domain
may attenuate the activity of the other. No doming activity was observed for the
following MCF7 cell lines: parent, Blank Vector, MT-1E, NT-1E, MT3ΔCT, or NT-CT-
1E (Table 1). The formation of domes in cell culture was observed in the following
MCF7 cell lines: WT MT-3, MT3ΔNT, and CT-1E (Table 1). In doming MCF7 cell
lines more domes per field of view were observed in cell lines possessing only the C-
terminal region of MT-3 (Figure 6). Domes were observed per one field of view that was
1.9 cm^2 using a 10x objective lens and the cellSens® microscope imaging software
(Olympus, MA).   A total of twenty one fields of view were observed for each doming
cell line and the number of observed domes (Figure 7). Overall an average of 51.89 +/-
7.89, 57.22 +/- 5.46, and 56.44 +/- 1.602 domes were observed when adding all twenty-
one fields of view for WT MT-3, MT-3ΔNT, and CT-1E MCF7 mutant cell lines
respectively (Table 1) (Figures 8-10). Domes per field of view averaged 2.69 for the CT-
1E cell line, wild type MT-3 had an average of 2.47 domes per field of view, and MT-
3ΔNT averaged 2.72 domes per field of view (Table 1).
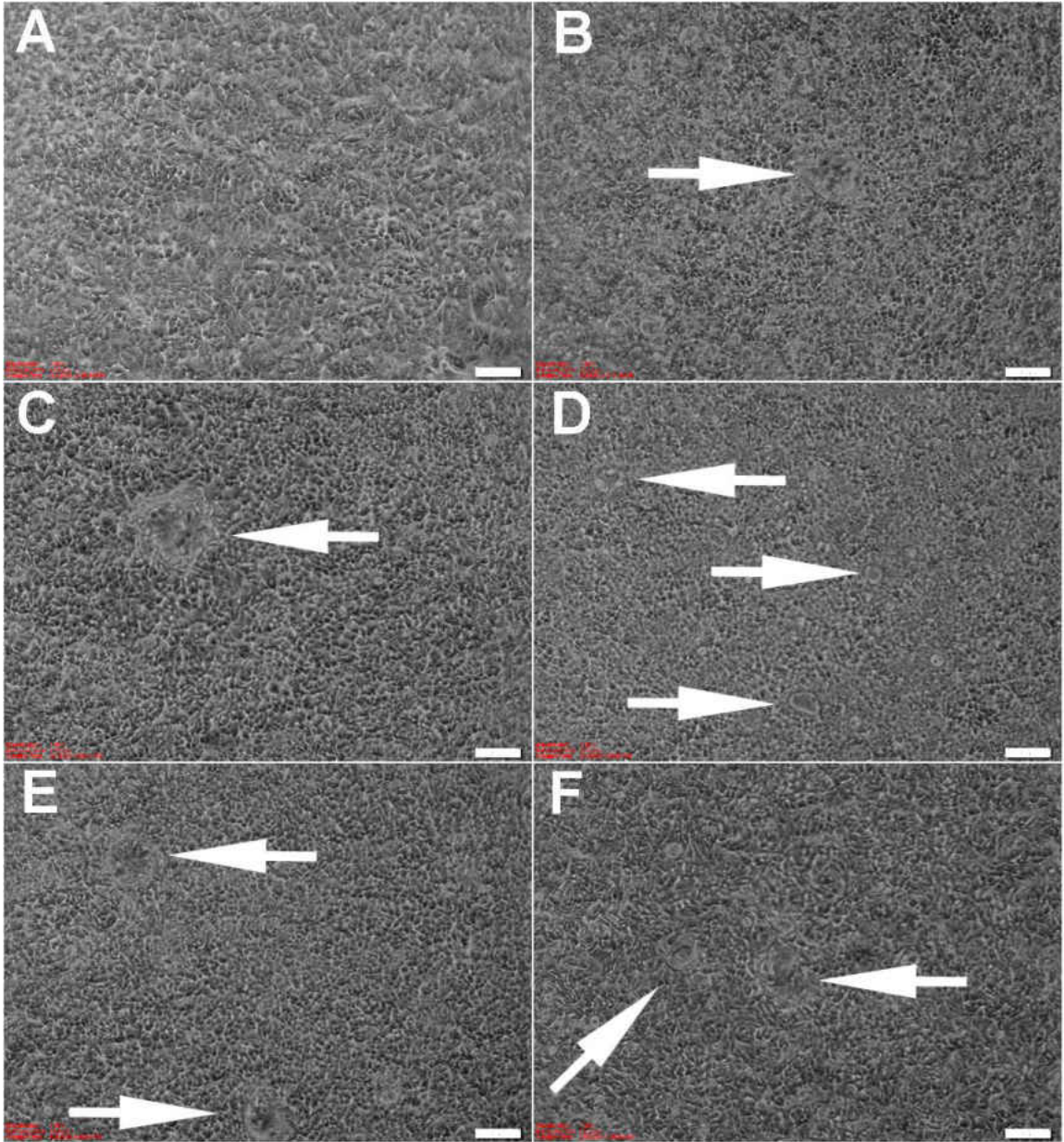
Figure 6: Images of MCF7 cells and MCF7 mutant cell lines doming in culture.

Domes are indicated by white arrows. A: MCF7 parent. B: MCF7 CT-1E. C and D:

MCF7 MT-3 cell line; C depicts a larger doming structure while D depicts several

smaller domes. E: MCF7 MT-3ΔNT. F: MCF7 MT-3ΔNT. Image taken 10 days after

cells were passaged and seeded at a 1:3 ratio. Magnification of 100x

Doming Observations

Figure 7: Domes observed per 21 fields of view in a T-25 cell culture flask. MCF7 WT MT-3 averaged 51.89 +/- 7.89 domes per flask, MT-3ΔNT averaged 57.22 +/- 5.46 domes per T-25 cell culture flask, and CT-1E averaged 56.44 +/- 1.60 domes per flask. Domes were not observed in the MCF7 parent, MT-3ΔCT, NT-1E, and MT-1E cell lines. No significant difference was determined among doming cell lines using the one-way ANOVA test.

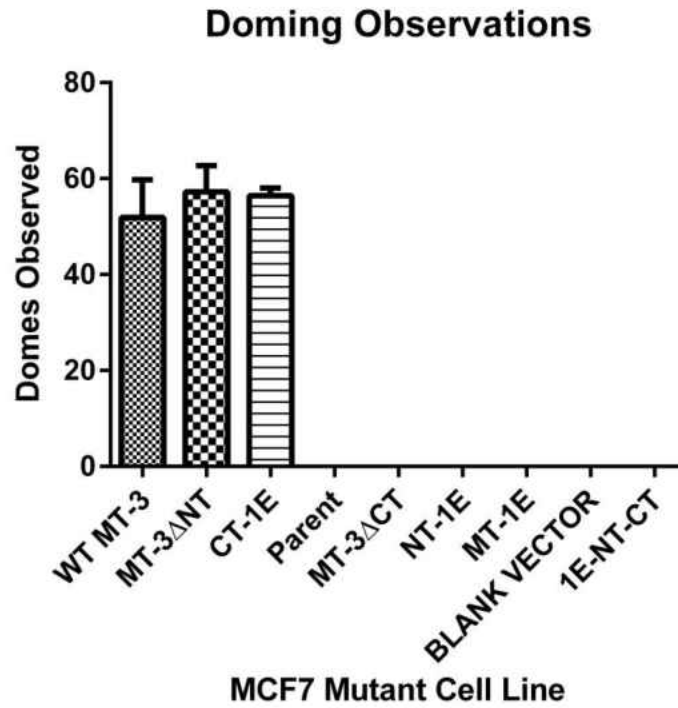| MCF7 Cell Line	Domes Observed in Cell Culture	Average Number of Domes Observed per Field of View	Average Number of Domes Observed per 21 Fields of View
WT MT-3	Yes	2.47	51.89
MT-3ΔNT	Yes	2.72	57.22
MT-3ΔCT	No	0	0
MT-1E	No	0	0
CT-1E	Yes	2.69	56.44
NT-1E	No	0	0
NT-CT-1E	No	0	0
Parent	No	0	0
Blank Vector	No	0	0

Table 1: Doming phenotype and domes observed for MCF7 mutant cell lines. Table indicates if domes were observed for each MCF7 mutant cell line. Average number of domes observed per field of view and per 21 fields of view for doming cell lines is also displayed.

Figure 8: Image of the MCF7 CT-1E mutant cell line depicting dome formation.

Domes appear as out of focus areas in relation to confluent cells still attached to the culture vessel, and are indicated by white arrows. Image taken 10 days after cells were passaged and seeded at a 1:3 ratio.   Magnification of 100x.
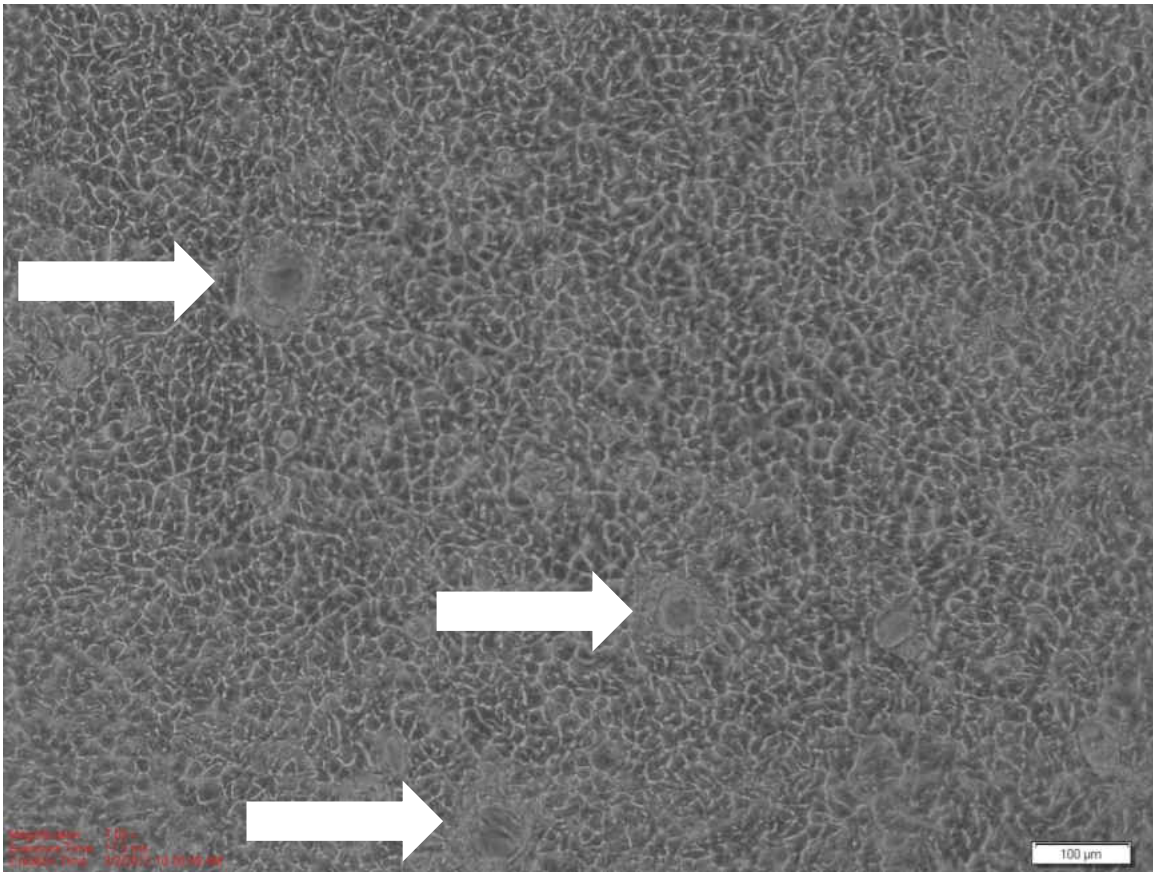
Figure 9: Image of the MCF7 WT MT-3 mutant cell line depicting dome formation.
Domes appear as out of focus areas in relation to confluent cells still attached to the
culture vessel, and are indicated by white arrows. Image taken 10 days after cells were
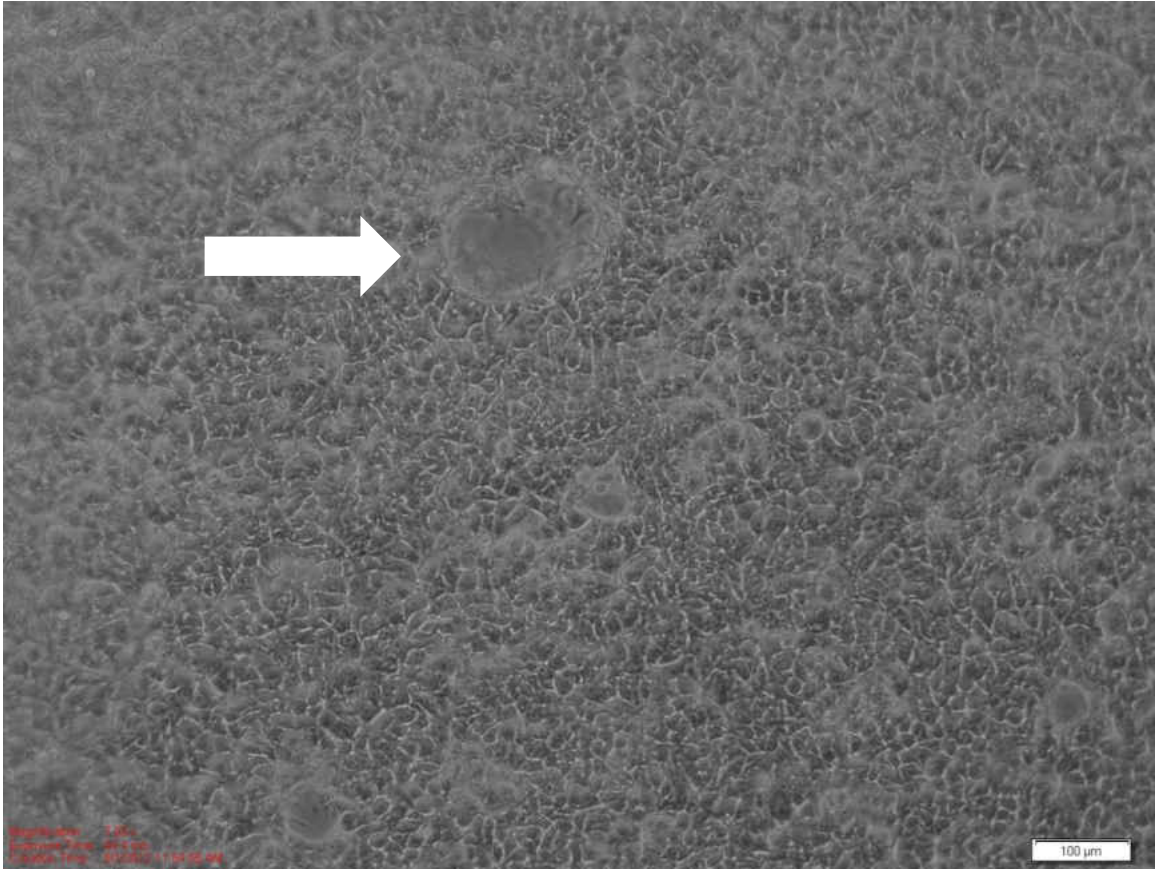passaged and seeded at a 1:3 ratio. Magnification of 100x.

Figure 10: Image of the MCF7 MT-3ΔNT mutant cell line depicting dome formation. Domes appear as out of focus areas in relation to confluent cells still attached to the culture vessel, and are indicated by white arrows. Image taken 10 days after cells were passaged and seeded at a 1:3 ratio.   Magnification of 100x.
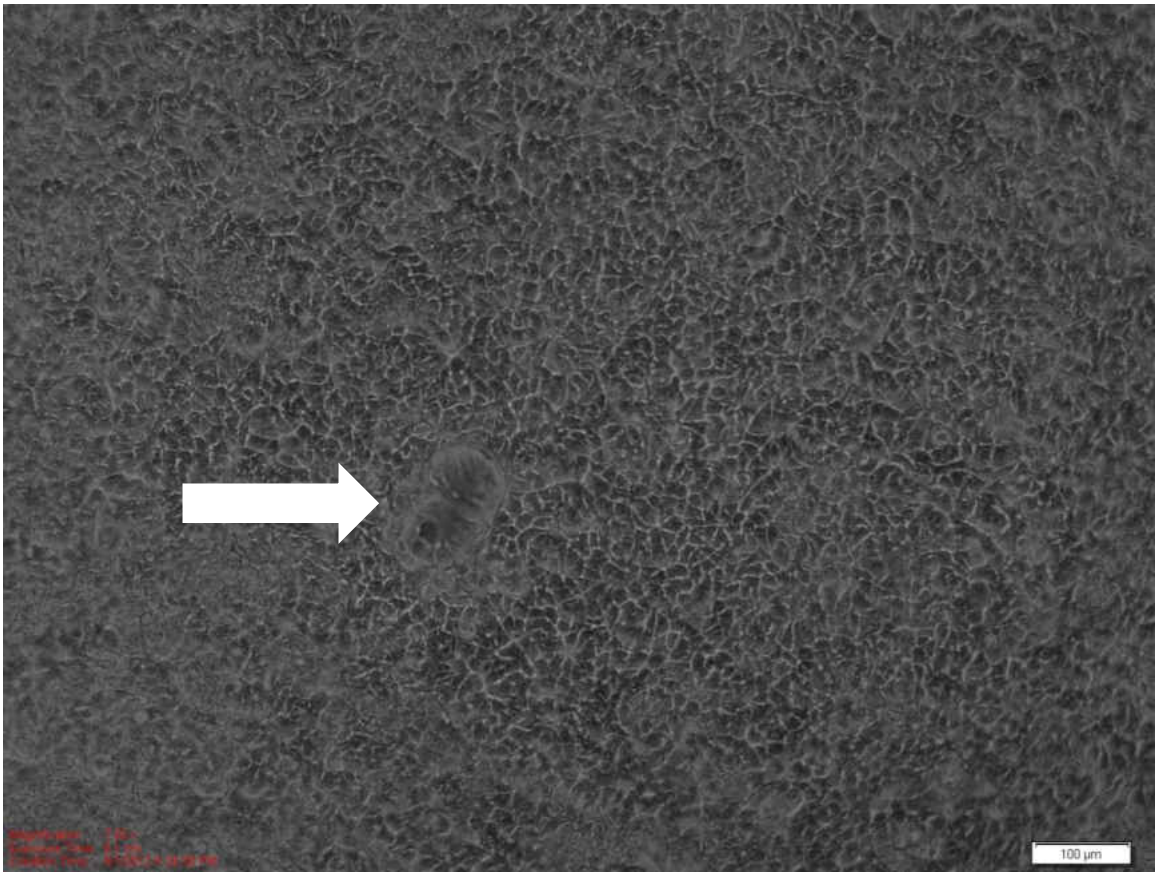
Doubling Times of MCF7 Cells Expressing Both or Either the N- and C-terminal Domains of MT-3

Metallothionein-3 is not expressed in normal breast epithelial cells, but is highly expressed in the majority of breast tumor samples (Sens et al. 2001). Expression of MT-3 in MCF7 or Hs 578T cells results in growth inhibition (Gurel et al. 2003) and increased chemotherapy drug resistance in MCF7 cells (Dutta et al. 2002). The role of MT-3 and its unique N- and C-terminal domains plays in the differentiation of breast cancer has yet to be fully described, and here we examine each domain's individual effect on MCF7's growth rate. MCF7 parent cells have a standard doubling time of 29 h (ATCC, MCF7), however in our laboratory we found that the doubling time for the MCF7 cells was 32.45 h. MCF7 cells expressing the MT-1E and Blank Vector construct had observed doubling times of 35.76 +/- 4.74 h and 39.51 +/- 5.96 h respectively. As a control group MCF7 parent, MCF7 MT-1E, and MCF7 Blank Vector had no statistically significant change in observed doubling times. MCF7 cell lines containing the following constructs WT MT-3, MT-3ΔNT, MT-3ΔCT, CT-1E, NT-1E, and NT-CT-1E had observed doubling times of 53.1 +/- 2.2, 57.31 +/- 3.83, 64.73 +/- 5.24, 55.28 +/- 11.25, 60.96 +/- 3.3, and 56.96 +/- 5.8 h respectively. All cell lines possessing the N-terminal region, C-terminal region, or both the N- and C-terminal regions of WT MT-3 had a doubling time that was observed to be significantly slower than the control cell lines parent MCF7, MT-1E, and Blank Vector (Figure 11).

MCF7 Mutant Cell Line Doubling Times
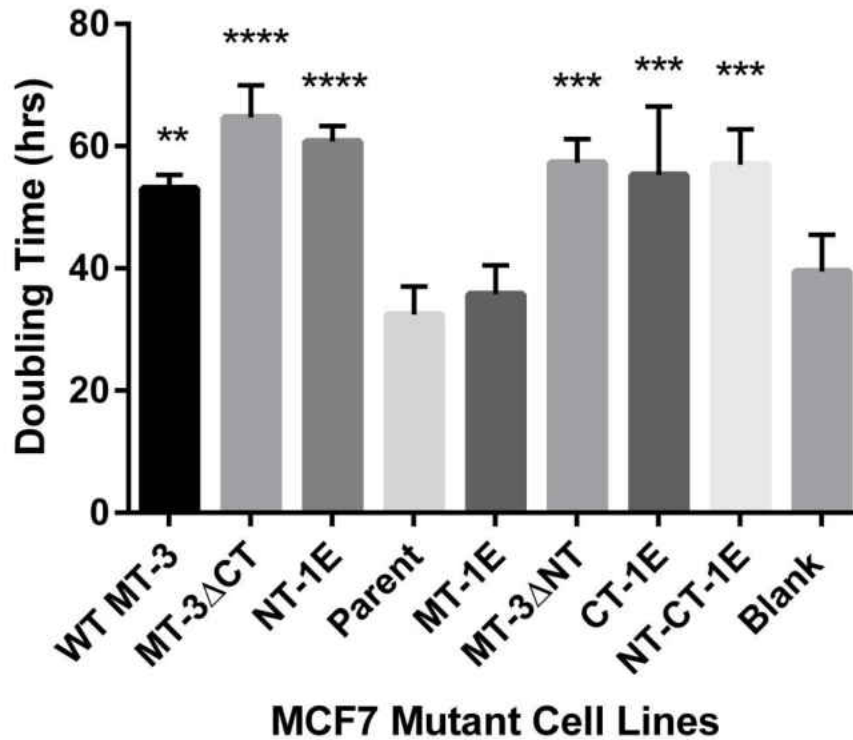
Figure 11: MCF7 mutant cell line doubling times. All mutant cell lines had increased doubling times in comparison to MCF7 parent except the MT-1E, and MCF7 Blank Vector cell lines. Statistical significance indicated by **, ***, or **** P-value less than 0.01, 0.001, and 0.0001 respectively using the one-way ANOVA followed by Tukey's posttest comparing all mutant cell lines to MCF7 Parent. Error bars represent SD. Three biological replicates were tested.

Evidence of a differentiated phenotype for cell lines possessing the C-terminal of MT-3 can be observed morphologically by the formation of domes in cell culture (Figures 6, 8, and 10) (Table 1), and by the increase in TER (Figure 12).

Transepithelial Resistance of MCF7 Cells Expressing Both or Either the N- and C-Terminal Domains of MT-3

The integrity and permeability of a cell monolayer can be measured using transepithelial resistance (TER). Measuring TER is a well-established method to determine the presence of tight junctions along with ionic permeability (Stevenson 1988). Expression of MT-3 in HK2 cells resulted in an increase in TER, dome formation, and the expression of E-cadherin indicating the formation and maintenance of cell to cell junctions characteristic of an epithelial cell (Bathula et al. 2008). Alterations in TER based on the N- or C-terminal of MT-3 were examined in MCF7 cells to determine if either domain or both contribute to the formation of a differentiated epithelial cell type.

The daily average TER on days five, six, and seven varied to a large degree amongst the MCF7 mutant cell lines (Table 2). This indicates that dome formation and the tight junctions associated with the epithelial phenotype may form and re-form as the monolayer is formed in MCF7 cells. The combined average TER on days five, six, and seven post-seeding were used to compare all MCF7 cell lines. The MCF7 parent cell line had a TER of 17.57 +/- 4.35 Ω/Cm^2 and WT MT-3 had the highest average TER of 48.72 +/- 6.79 Ω/Cm^2. MCF7 cell lines MT-1E, Blank Vector, MT-3ΔNT, MT-3ΔCT, CT-1E, NT-1E, and NT-CT-1E had TER averages from days five to seven post seeding of: 33.17 +/- 1.47, 21.64 +/- 5.62, 47.58 +/- 5.55, 32.87 +/- 5.62, 30.09 +/- 4.35, 34.72 +/- 2.67, and 51.19 +/- 7.75 Ω/Cm^2 respectively (Table 2). It was observed that TER over seven days

of measurements was typically higher for cells possessing the C-terminal domain of MT-3 (Figure 12). When compared to the MCF7 parent cell line WT MT-3, MT-3ΔNT, and NT-CT-1E mutant cell lines had a significant increase in TER. The average TER from day 5 indicated no significant increase using the MCF7 parent cell line as the control (Figure S3), in the case of day 6 the NT-CT-1E cell line had a significant increase in TER in comparison to the parent cell line (Figure S4). On day 7 the WT MT-3, MT-3ΔNT, and NT-CT-1E had significantly increased TER measurements in comparison to the MCF7 parent cell line (Figure S5).

Figure 12: **Average TER from days 5, 6, and 7 post seeding on trans-well inserts.**
Each MCF7 mutant cell line is represented on the x axis, while the calculated TER is
displayed on the y axis. Increased TER is indicative of the formation of tight junctions,
and is associated with the doming phenotype. Statistical significance indicated by ** P-
value less than 0.01 using the one-way ANOVA test and Dunnet's posttest for multiple
comparisons using the MCF7 parent cell line as a control. Error bars represent SD.
Three biological replicates were tested.

MCF7 Cell Line	Average TER Day 5 (Ω/Cm²)	Average TER Day 6 (Ω/Cm²)	Average TER Day 7 (Ω/Cm²)	Average TER Day 5, 6, and 7 (Ω/Cm²)
WT MT-3	35.32 +/- 5.81	53.57 +/- 13.88	52.27 +/- 12.11	48.72 +/- 6.79
MT-3ΔNT	41.99 +/- 9.26	53.08 +/- 9.57	47.67 +/- 5.16	47.58 +/- 5.55
MT-3ΔCT	26.39 +/- 1.99	44.06 +/- 3.37	28.16 +/- 5.87	32.87 +/- 5.62
MT-1E	32.68 +/- 7.26	35.92 +/- 6.98	30.91 +/- 8.41	33.17 +/- 1.47
CT-1E	22.96 +/- 11.94	29.34 +/- 9.40	37.98 +/- 7.07	30.09 +/- 4.35
NT-1E	37.58 +/- 10.23	34.3 +/- 9.4	32.28 +/- 12.61	34.72 +/- 2.67
NT-CT-1E	37.91 +/- 12.10	64.76 +/- 5.95	50.91 +/- 14.26	51.19 +/- 7.75
Parent	18.80 +/- 1.46	22.27 +/- 4.63	8.96 +/- 1.92	17.57 +/- 4.35
Blank Vector	41.99 +/- 5.38	27.38 +/- 10.76	36.80 +/- 6.48	35.39 +/- 5.62

Table 2: Average TER for MCF7 mutant cell lines for days 5, 6, and 7. Table indicates the average TER for each MCF7 mutant cell line for days 5, 6, and 7 expressed as Ω/Cm^2 and indicating the SEM. The combined average TER of days 5, 6, and 7 is used to evaluate the relationship between TER and the presence or absence of the N- and C-terminal of MT-3. Three biological replicates were tested.

Microarray Analysis of MCF7 Cells Expressing Both or Either the N- and C-terminal Domains of MT-3

The function of WT MT-3 and its N- and C-terminal domains in the differentiation of breast cancer remains to be fully elucidated. Microarray analysis and subsequent investigation into differentially expressed genes (DEGs) could indicate important cellular pathways that become altered based on the presence or absence of WT MT-3 and its unique N-and C-terminal domains. All the MCF7 mutant cell lines, except NT-CT-1E, underwent microarray analysis in order to determine DEGs. Overlap hierarchical clustering demonstrates that the N- and C-terminal domains have unique expression relationships based on clustering dendrogram (Figure 13). Mutants possessing either the N- or C-terminal regions also grouped together on the clustering dendrogram suggesting a similar pattern of gene expression among cell lines containing the same terminal regions (Figure 13). Differentially regulated genes from microarray analysis that were significantly altered compared to Blank Vector as a control include: NELL2, PAPSS2, PYGL, VGSC, and LRRC49. The GAGE antigen family was also found to be differentially regulated on the microarray uniquely by the N- or C-terminal domains of MT-3.
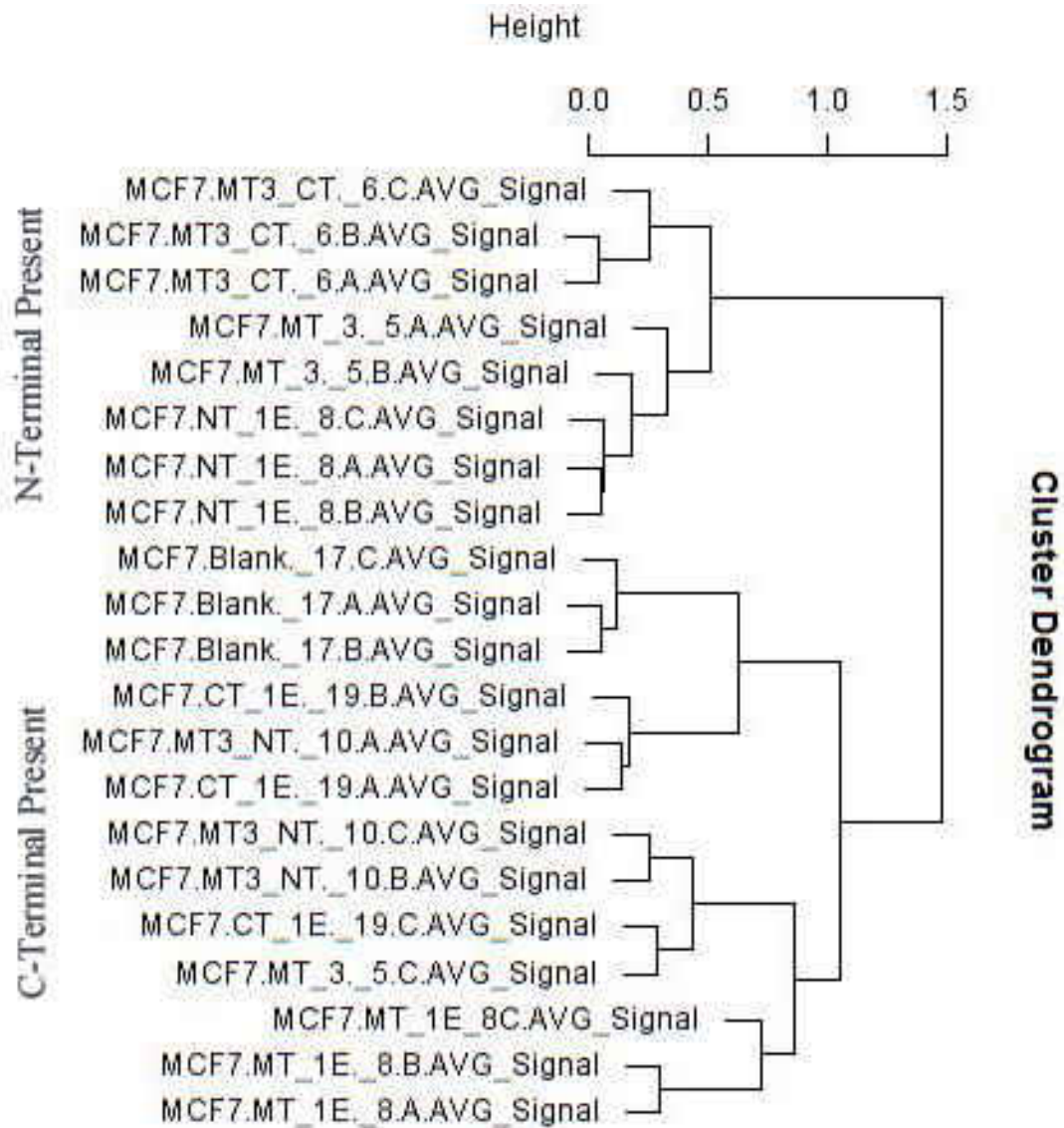
Figure 13: Cluster dendrogram of MCF7 mutant cell lines. Clustering determined using the Overlap Hierarchal Clustering based on differentially expressed genes. Clustering demonstrates that cells possessing the N- or C-terminal took residence in different areas of the diagram. The proximity of one cell line to another indicates the degree of difference in gene expression. Closer cell lines being more similar and further being more different.

Differential Expression Analysis of LRRC49, NELL2, PAPSS2, PYGL, VGSC, and MMP-1 in MCF7 Cells Expressing Both or Either the N- and C-terminal Domains of MT-3

Microarray analysis indicated that LRRC49 expression had a 4.46 fold increase in the MCF7 WT MT-3 cell line, a 4.35 fold increase in the MCF7 MT-3ΔNT cell line, a 5.53 fold increase in the NT-1E cell line, and a 1.54 fold increase in the CT-1E cell line. Expression of the NELL2 gene in MCF7 MT-3ΔNT and CT-1E mutant cell lines was induced by 1.2 fold and 1.07 fold respectively. In the MCF7 WT MT-3, MT-3ΔNT, and CT-1E cell lines PAPSS2 expression was increased 1.22, 1.55, and1.35 fold respectively. Repression of PYGL occurred in the MCF7 MT-3ΔNT and CT-1E mutant cells lines where expression was .98 and .83 of the control respectively. The VGSC family member SCNN1A was upregulated 2.35 fold in the MCF7 NT-1E cell line. The previously mentioned genes underwent validation using qualitative real time PCR and were normalized to beta actin. Validation data indicated that none of the genes were significantly up or down-regulated in any of the MCF7 mutant cell lines. Based on microarray data from the HK2 MT-3 cell line, MMP-1 was also investigated in all the MCF7 mutant cell lines. Qualitative real time PCR demonstrated that MMP-1 was significantly up-regulated 5.33 fold in the MCF7 NT-CT-1E cell line (Figure 14) using MCF7 Blank Vector as the control.
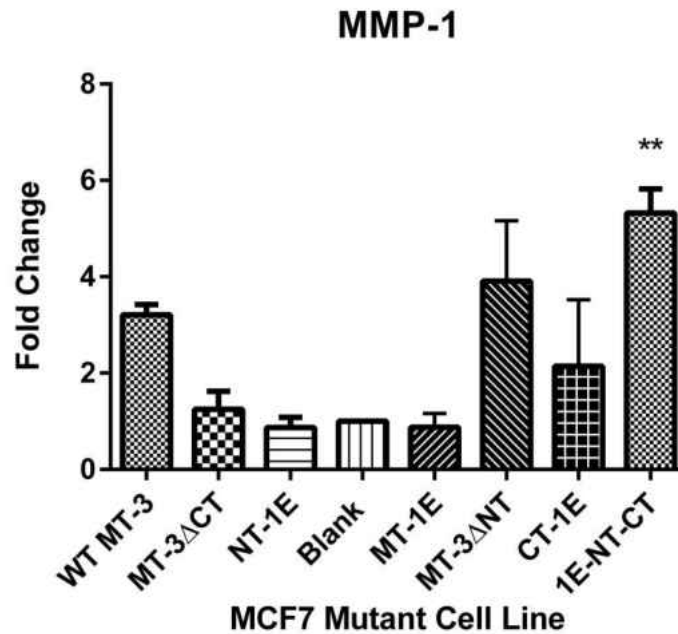
Figure 14: Fold change in expression of the MMP-1 in MCF7 mutant cell lines. Data

suggests that the presence of MT-3 may increase the expression of MMP-1 as indicated

by the significant increase in expression of MMP-1 in the MCF7 NT-CT-1E mutant cell

lines when compared to the MCF7 Blank Vector and MT-1E cell lines. Statistical

significance indicated by ** P-value less than 0.01. Significance determined using one-

way ANOVA and Dunnet's posttest. Error bars represent SD. Three biological

replicates were tested.

GAGE Family Antigens are Differentially Expressed Based on the Presence or Absence of the N- and C-terminal Domains of MT-3

Recent evidence suggests that the GAGE family antigens may direct cell proliferation, differentiation, and the survival of germ line cells (Simpson et al. 2005). To determine if the N- or C-terminal of MT-3 can differentially regulate genes, the microarray was examined for genes up- or down-regulated by one terminal being present and the opposite effect happening for the other terminal. The GAGE family antigens were found to be down-regulated by WT MT-3 and when the N-terminal-only mutants, NT-1E and MT-3ΔCT, were present (Figures 15-22). For several GAGE family antigens when the C-terminal-only cell line CT-1E was present expression significantly increased (Figures 15-22) in comparison to the Blank Vector cell line. The microarray analysis indicated that GAGE12H, GAGE12G, GAGE6, and GAGE12F were differentially regulated by the N- or C-terminal of MT-3. Additional GAGE family antigens were also tested by real time PCR. Genes that were validated include GAGE12H, GAGE12G, GAGE4, GAGE5, GAGE6, GAGE2C, GAGE2E-1, and GAGE2E-2. Due to a suitable primer being unavailable GAGE12F was not validated.

Using the MCF7 Blank Vector as a control, the relative changes in expression were determined from the microarray for the GAGE antigen family. The MCF7 WT MT-3 cell line had repression of GAGE12H, GAGE12G, and GAGE6 to 0.93, 0.82, and 0.85 respectively. In the MCF7 MT-3ΔNT GAGE12F was upregulated 1.45 fold. The MCF7 MT-3ΔCT cell line had repression of GAGE12H, GAGE12G, GAGE4, GAGE5, GAGE6, and GAGE12F to 0.52, 0.41, 0.46, 0.47, 0.43, and 0.62 respectively. Repression was again seen the N-terminal containing MCF7 NT-1E cell line where GAGE12H, GAGE12G, GAGE4, and GAGE6 expression levels were 0.66, 0.58, 0.64,

and 0.63 respectively of control. For the C-terminal containing MCF7 CT-1E cell line there was an increase in expression for GAGE12H, GAGE12G, GAGE5, and GAGE12F genes of 2.55, 2.78, 2.93, and 3.27 respectively of control. The GAGE12F gene was the only GAGE family antigen appearing on the microarray for the MCF7 MT-1E cell line and was up-regulated 1.23 fold.

Validation of the GAGE family antigens using real time PCR confirmed a pattern of up regulation in the presence of the MCF7 CT-1E cell line for the majority tested. The GAGE2C, GAGE5, and GAGE12H were all significantly down-regulated in MCF7 WT MT-3, MT-3ΔCT, and NT-1E cell lines. Those same genes were all significantly upregulated in MCF7 MT-1E and CT-1E mutant cell lines (Figures 15, 16, and 19). The N-terminal cell lines MCF7 MT-3ΔCT and NT-1E along with WT MT-3 had the GAGE2E-2, GAGE6, and GAGE2E-1 genes significantly down-regulated (Figures 15, 16, and 18). For the MCF7 mutant cell lines containing the C-terminal GAGE2E-1 was significantly up-regulated in the MT-3ΔNT cell line (Figure 16), as was GAGE12G (Figure 20) and GAGE2E-2 (Figure 17). Validation indicated that GAGE4, GAGE12G, and GAGE2E-2 were all significantly upregulated in the MCF7 cell lines expressing MT-1E and CT-1E (Figures 16, 18, and 21). The GAGE6 antigen was also significantly up-regulated in the MCF7 CT-1E mutant cell line (Figure 19).
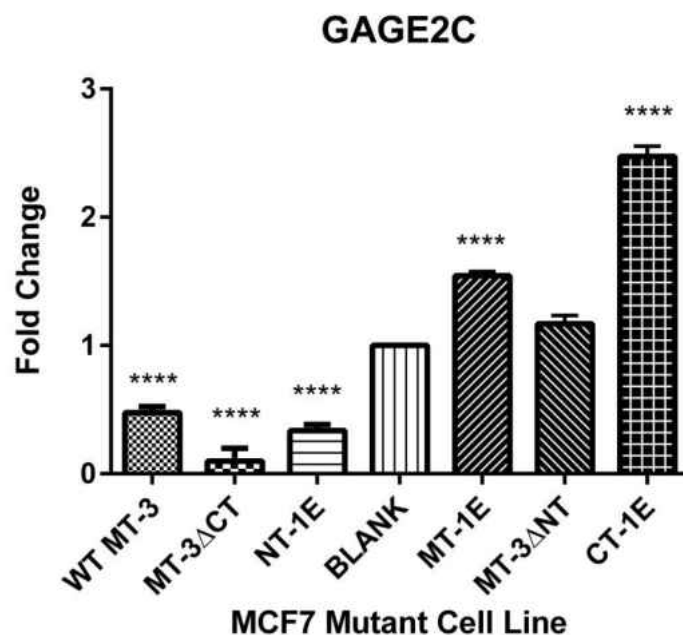
Figure 15: Expression of GAGE2C gene in various MT mutants in MCF7 cells.

Fold change in expression of the GAGE2C antigen in MCF7 mutant cell lines using

Blank Vector as the control. Statistical significance indicated by **** P-value less than

0.0001. Significance determined using one-way ANOVA and Tukey's posttest. Error

bars represent SEM. Three biological replicates were tested.

Figure 16: Fold change in expression of the GAGE2E-1 antigen in MCF7 mutant cell lines. Changes in fold expression were measured using MCF7 blank vector as the control. Statistical significance indicated by ** or **** P-value less than .01, .0001 respectively. Significance determined using one-way ANOVA and Tukey's posttest. Error bars represent SEM. Three biological replicates were tested.

GAGE2E-2

Figure 17: Fold change in expression of the GAGE2E-2 in MCF7 mutant cell lines.

Changes in fold expression were measured using MCF7 blank vector as the control.

Statistical significance indicated by *, ***, or **** P-value less than .05, .001, and .0001

respectively. Significance determined using one-way ANOVA and Tukey's posttest.

Error bars represent SEM. Three biological replicates were tested.

GAGE4

Figure 16: Fold change in expression of the GAGE4 in MCF7 mutant cell lines.
Changes in fold expression were measured using MCF7 blank vector as the control.
Statistical significance indicated by ** or **** P-value less than .01, and .0001
respectively. Significance determined using one-way ANOVA and Tukey's posttest.
Error bars represent SEM. Three biological replicates were tested.
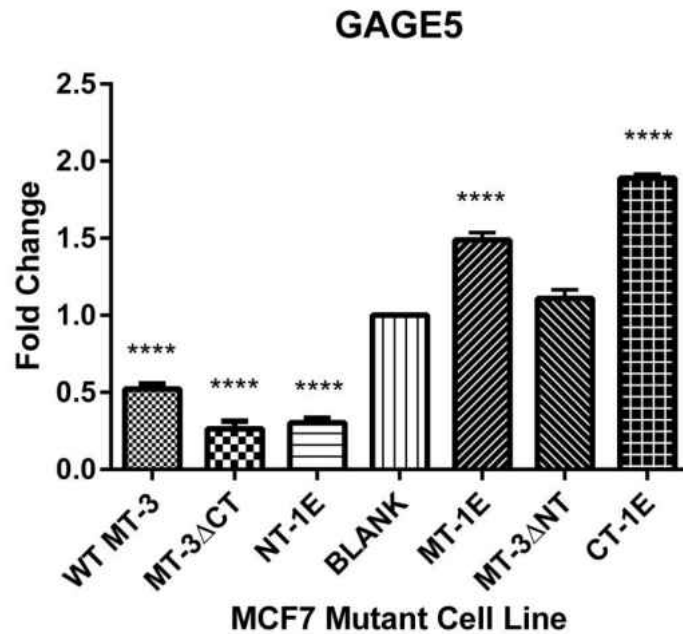
Figure 19: Fold change in expression of the GAGE5 in MCF7 mutant cell lines.

Changes in fold expression were measured using MCF7 blank vector as the control.

Statistical significance indicated by **** P-value less than .0001. Significance

determined using one-way ANOVA and Tukey's posttest. Error bars represent SEM.

Three biological replicates were tested.
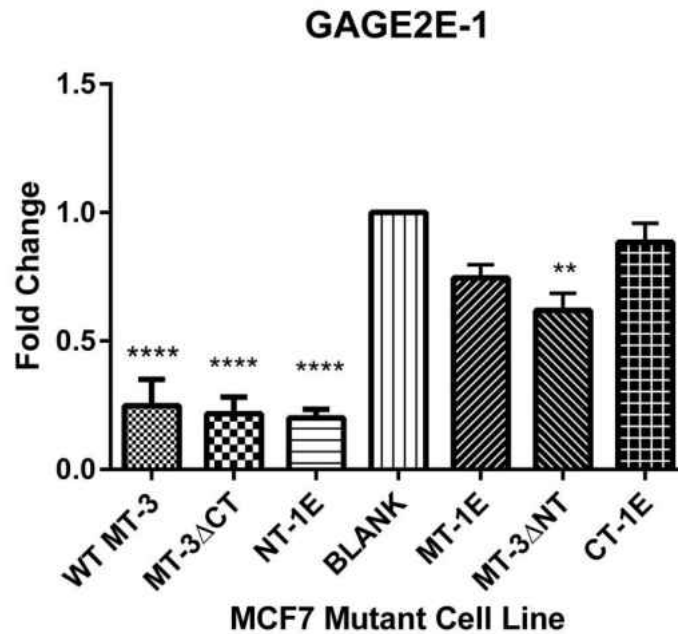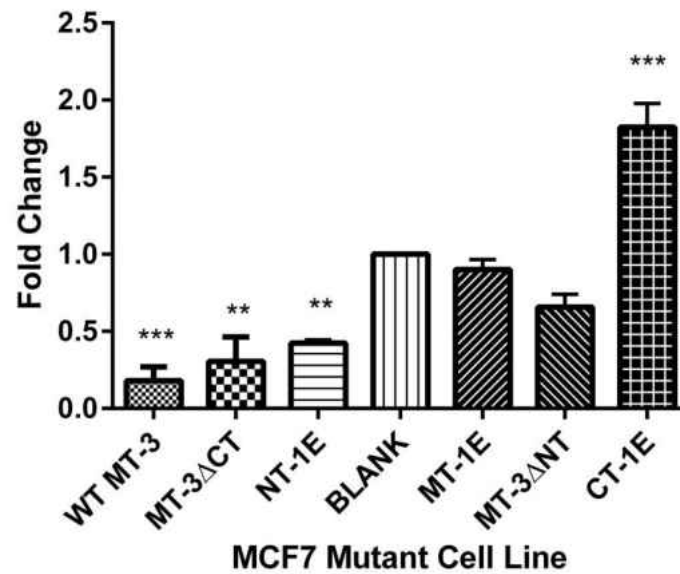
Figure 20: Fold change in expression of the GAGE6 in MCF7 mutant cell lines.

Changes in fold expression were measured using MCF7 blank vector as the control.

Statistical significance indicated by ** or *** P-value less than .01, and .001

respectively. Significance determined using one-way ANOVA and Tukey's posttest.

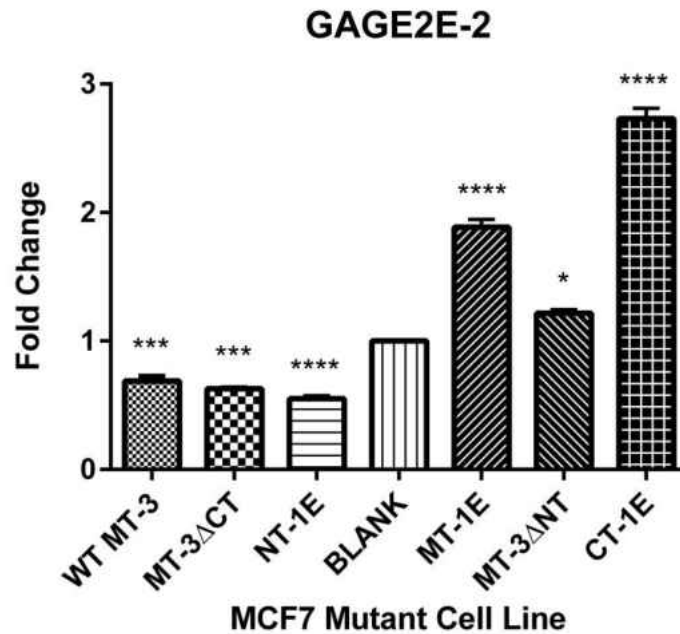Error bars represent SEM. Three biological replicates were tested.
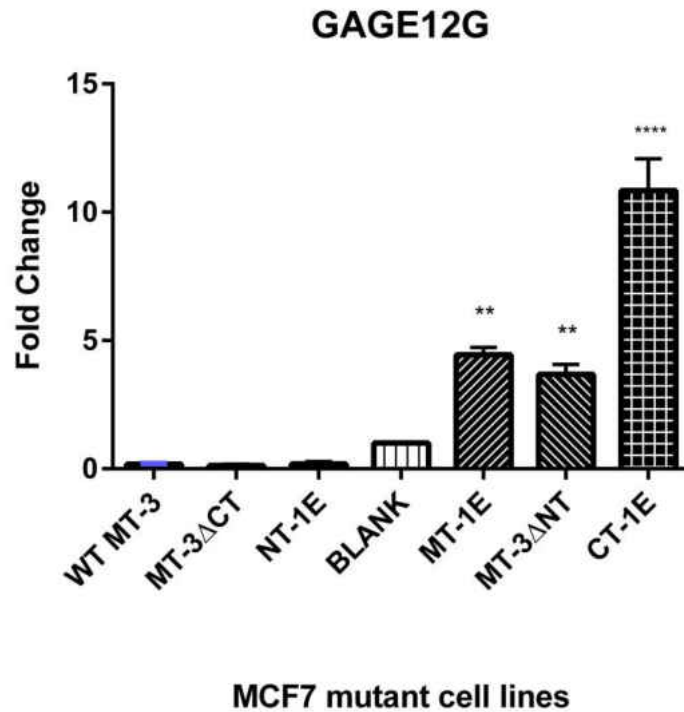
Figure 21: Fold change in expression of the GAGE12G in MCF7 mutant cell lines.

Changes in fold expression were measured using MCF7 blank vector as the control.

Statistical significance indicated by ** or **** P-value less than .01, and .0001

respectively. Significance determined using one-way ANOVA and Tukey's posttest.

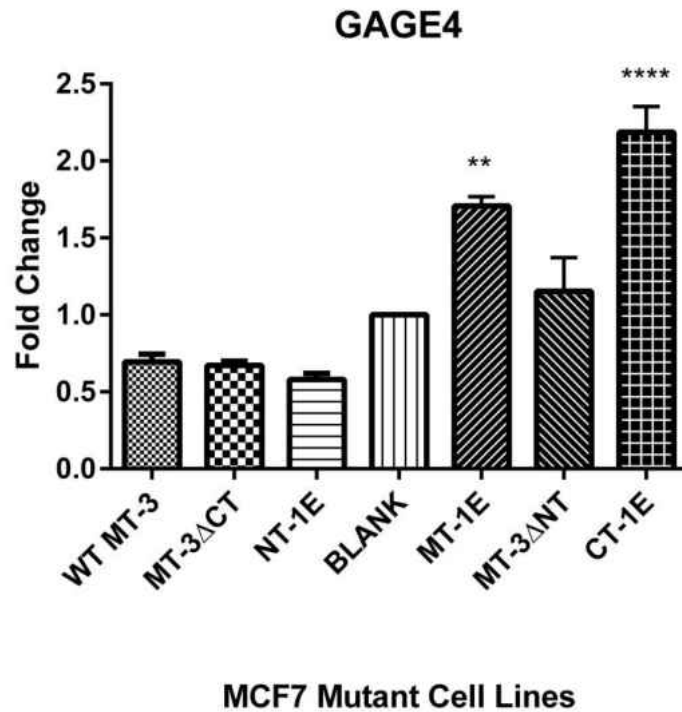Error bars represent SEM. Three biological replicates were tested.
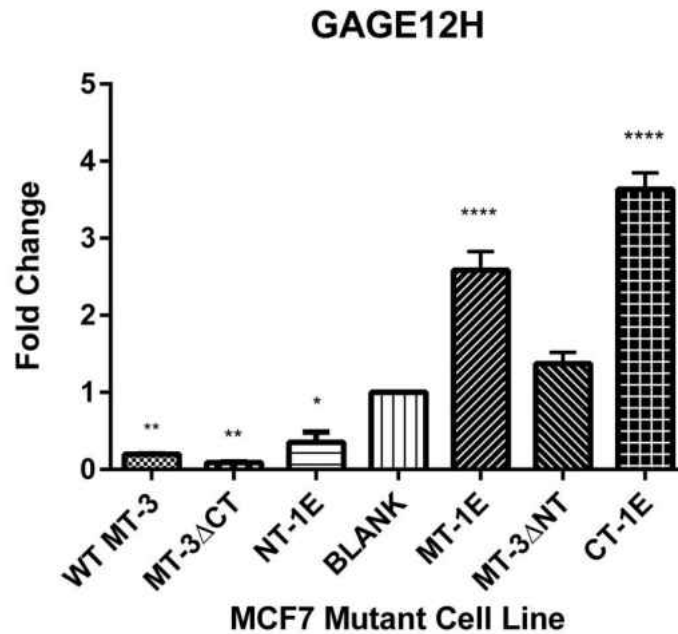
Figure 22: Fold change in expression of the GAGE12H in MCF7 mutant cell lines.
Changes in fold expression were measured using MCF7 blank vector as the control.
Statistical significance indicated by *, **, or **** P-value less than .05, .01, and .0001
respectively. Significance determined using one-way ANOVA and Tukey's posttest.
Error bars represent SEM. Three biological replicates were tested.

CHAPTER IV

DISCUSSION

The Role of MT-3 in Transcriptional Regulation of E-cadherin

A hallmark of the transition between epithelial and mesenchymal cell types is in the inverse expression of E- and N-cadherin (Bathula et al. 2008). Loss of E-cadherin expression is one of the events prior to a cell becoming mesenchymal, while induction of E-cadherin is needed for the formation of adherens junctions and a complete epithelial layer. The HK2 cell line has no basal expression of MT-3 and is non-doming; however restoration of MT-3 expression increases E-cadherin expression and creates a doming phenotype (Bathula et al. 2008). Transcriptional regulation of E-cadherin has also been shown be repressed by the E-box binding transcription repressors Slug and Snail (Batlle et al. 2000). Transcription repressors Slug and Snail bind E-box elements CAGGTG, TCACCTG, and CACCTG and mutation of those sequences to AACCTA, AACCTA, and AACCTA prevents the binding and E-cadherin expression increases (Batlle et al. 2000). The role of MT-3 in the regulation of E-cadherin expression was examined using a WT E-cadherin promoter and one with four mutated E-boxes. Expression of MT-3 in HK2 cell lines caused a significant increase in the expression of E-cadherin in the case of the WT promoter and the promoter containing mutated E-boxes (Figure 5). The presence of MT-3 appears to have an additive effect increasing the expression of E-cadherin

beyond the baseline expression for the construct containing the mutated E-boxes. If MT-3 functioned to regulate E-cadherin expression by interacting with E-box elements it would be expected that the expression would not increase once the E-box elements had been mutated. Data suggest that 36 hours post-transfection MT-3 up-regulates E-cadherin expression and this is not wholly mediated by E-box repression. It is likely that MT-3 is indirectly up-regulating E-cadherin expression and not independently interacting with the promoter.

The Role of MT-3 in MCF7 Cell Differentiation

Studies have demonstrated that MT-3 is involved in the maintenance of vectorial active ion transport in human proximal tubule cells (Kim 2002), and that restoration of MT-3 expression in HK2 cells confers the doming phenotype (Bathula et al. 2008). The doming phenotype indicates that cell cultures derived from transporting epithelial cells have retained vectorial active transport activity (Lever, 1985). Domes appear in cell culture vessels as out of focus in relation to the monolayer indicating they are raised and detached from the cell culture vessel due to water following transported ions in the basolateral surface. This study demonstrated that MCF7 cells differentiated into a doming phenotype when the C-terminal of MT-3 was present (Figures 6, 8, 9 and 10). Cell lines able to form domes had no significant difference in the visible doming activity when compared to other cell lines possessing the doming phenotype (Figure 7). Utilizing TER measurements is an established method to determine the presence of tight junctions and ionic permeability of the cell monolayer (Kang et al. 2015). Transepithelial resistance measurements were significantly higher in the MCF7 mutant cell lines WT

MT-3, MT-3ΔNT, and NT-CT-1E when compared to the parent MCF7 cell and the MT-1E cell line (Figure 12). The findings indicate that the C-terminal of MT-3 may be responsible for the formation of tight junctions and conferring the doming phenotype, but that the C-terminal alone may not lead to significant increase in TER as indicated by the MCF7 mutant cell line CT-1E (Figure 12).

The N-terminal of MT-3 contains a Thr residue that is not present in any of the other MT isoforms (Andrews 2000; Aschner et al. 1997; Kagi and Hunziker 1989). It has been demonstrated that this Thr is responsible for the growth inhibitory activity associated with MT-3 (Kagi and Hunziker 1989). Addition of MT-3 to cultured rat cortical neurons inhibits survival and neurite outgrowth, and elevating the expression of MT-3 in rat C-6 glial cells also confers growth inhibitory activity (Tsuji et al. 1992). This growth inhibitory activity is unique to MT-3 and despite a 63-69% sequence identity no other MT isoforms confer growth inhibition (Aschner et al. 1997). The growth inhibitory activity of MT-3 also occurs in MCF7 and Hs578T cells, but not to the MDA-MB-231 and T-47D cell lines (Gurel et al. 2003c). This study examined the doubling time of MCF7 cells expressing WT MT-3, MT-1E, and mutant forms containing either the N-terminal or C-terminal domains of MT-3 and both the N- and C-terminal of MT-3 (Figure 3). The MCF7 WT MT-3, MT-3ΔNT, MT-3ΔCT, CT-1E, and NT-1E cell lines had a significant increase in doubling time in comparison to the parent MCF7 cell line and Blank Vector (Figure 11). The MCF7 MT-1E cell line did not have a significant change in doubling time when compared to the parent MCF7 and Blank Vector cell lines. The growth inhibition of cell lines containing the C-terminal of MT-3 but not the N-terminal may be due the C-terminal domain initiating differentiation of the cell line into a

more epithelial phenotype as indicated by dome formation in cell culture (Figures 6-10) and increased TER (Figure 12).

Overexpression of MT-3 occurs in breast cancers and esophageal cancers (Somji et al. 2010; Tian et al. 2013) that have a poor prognosis. The presence of MT-3 may serve as a protective mechanism inhibiting cellular proliferation by altering the expression of other genes (Tian et al. 2013). Microarray analysis and overlap hierarchical clustering implicated that there were unique alterations in gene expression based on the presence or absence of the N- or C-terminal of MT-3 (Figure 13). Further investigation of up or down-regulated genes based on the microarray included: PAPSS2, MMP-1, LRRC49, NELL2, PYGL, VGSCs, and the family of GAGE antigens. The protein LRRC49 has been shown to have elevated expression levels in ER+ breast cancers compared to ER- breast cancers (De Souza Santos et al. 2008), and NELL2 is over expressed in Burkitt's lymphoma and in neuroblastomas (Maeda et al. 2001). Overexpression of PAPSS2 in MCF7 cells has been shown to slow cellular proliferation by arresting cell cycle progression and inducing apoptosis (Xu et al. 2012), while down regulation of PYGL can cause cancer cells to undergo senescence (Favaro et al. 2012). Expression of the VGSCs Nav1.6 and Nav 1.7 occurs in prostate cancer cell lines and other metastatic cells (Shan et al. 2014). Although significant alterations in expression of NELL2, PAPSS2, PYGL, VGSCs, and LRRC49 was indicated by microarray analysis real time PCR indicated there was no significant changes in expression for those genes in comparison to MCF7 Blank Vector as a control. During carcinogenesis MMPs act as mediators of alterations observed in the microenvironment during both early and late stages of disease progression (Yadav et al. 2014). The MCF7 mutant cell line NT-CT-1E

had a significant increase in the expression of MMP-1 using MCF7 Blank Vector as a control (Figure 14). An over-expression of MT-3 and subsequent increased expression of MMP-1 may be indicative of disease progression.

The N-and C-terminal of MT-3 Differentially Regulate the Expression of GAGE Antigens

The exact biological function of the GAGE antigens remains unknown recent evidence suggests that they may direct cell proliferation, differentiation, and the survival of germ line cells (Simpson et al. 2005), additionally antiapoptotic properties have also been attributed to GAGE antigens (Cilensek et al. 2002). The presence of GAGE antigens in various aggressive carcinomas makes any alteration in expression of interest (Cheung, Chi, Cheung 2000; Kong et al. 2004; Zambon et al. 2001). Microarray analysis indicated that the expression of GAGE antigens in MCF7 mutant cell lines was down-regulated when the N-terminal of MT-3 was present and up-regulated when the C-terminal alone was present. Real time PCR on several family members of the GAGE antigens supported that finding (Figures 15-22).

Data suggests that the presence of the N-terminal of MT-3 may repress the expression of GAGE2C and GAGE2E-1 as indicated by the significant reduction in expression of GAGE2C and GAGE2E-1 in WT MT-3, MT-3ΔCT, and NT-1E MCF7 cell lines (Figures 15-16). Lack of the N-terminal restores expression of GAGE2E-1 to control levels with the exception of the MT-3ΔNT mutant cell line which exhibits repression in comparison to the blank vector cell line (Figure 16). Real time PCR suggests that the presence of the N-terminal of MT-3 may repress the expression of GAGE2E-2 since there is significant reduction in expression of GAGE2E-2 in WT MT-3,

MT-3ΔCT, and NT-1E (Figure 17). The presence of any MT lacking the N-terminal of MT-3 may induce the expression of GAGE2E-2 as indicated by the MT-1E, MT-3ΔNT, and CT-1E mutant cell lines which exhibit increased expression in comparison to the Blank Vector cell line (Figure 17). The C-terminal of MT-3 may induce the expression of GAGE4 and GAGE5 as indicated by the significant increase in expression of GAGE4, GAGE 5, and GAGE12H in the MCF7 CT-1E cell line (Figures 18, 19, 22). Metallothioneins may also induce GAGE4, GAGE5, and GAGE12H antigen expression as indicated by the increase seen in the MT-1E cell line (Figures 18, 19, 22). The presence of the N-terminal of MT-3 may repress the expression of GAGE5 as indicated by the significant reduction in expression of GAGE5 in WT MT-3, MT-3ΔCT, and NT-1E MCF7 cell lines (Figure 19). Data suggests that the presence of the C-terminal of MT-3 may induce the expression of GAGE6 as indicated by the significant increase in expression of GAGE6 in CT-1E cell line. The N-terminal of MT-3 may be responsible for repressing the expression of GAGE6 since WT MT-3, MT-3ΔCT, and NT-1E all have decreased levels of GAGE6 mRNA (Figure 20). Expression of GAGE12G had a significant increase in expression in MT-1E, MT-3ΔNT, and CT-1E MCF7 mutant cell lines (Figure 21). The N-terminal of MT-3 may be responsible for repressing the expression of GAGE12H since WT MT-3, MT-3ΔCT, and NT-1E all have suppressed levels of GAGE12H mRNA in those cell lines (Figure 22).

Wild type MT-3 consistently down-regulated GAGE antigen expression despite having both the N- and C-terminals present suggesting that the N-terminal of MT-3 was actively altering gene expression in the MCF7 cell line. The GAGE antigens were often up-regulated in the MCF7 CT-1E mutant cell line as was the MCF7 MT-1E cell line.

This may indicate the metallothioneins may differentially up regulate GAGE antigen expression, while the N-terminal of MT-3 is able to down regulate expression of those same antigens.

Increased expression of E-cadherin is indicative of an epithelial phenotype while the over-expression of N-cadherin coupled with down-regulation of E-cadherin indicates a transition to a more mesenchymal state. Data indicates that in the HK2 cell line expression of MT-3 re-establishes the expression of E-cadherin and subsequently the cells differentiate into an epithelial phenotype. Data from this study suggests that MT-3 up regulates E-cadherin expression independent of E-box elements and most likely indirectly from E-cadherin promoter itself. No alteration in the expression of E-cadherin and N-cadherin occurred in the MCF7 mutant cell lines as indicated by RT-PCR (data not shown). However, the MCF7 cell line is known to maintain an epithelial phenotype.

The downstream effects of MT-3 expression in the progression and differentiation of breast cancer are many, and could be dependent on which region, the N- or C-terminal, is active. The antiapoptotic properties of GAGE antigens along with their potential involvement in cell proliferation, survival of germline cells and differentiation correlates to a role in cancer that allows the tumors to divide and survive. Data suggests that the N-terminal region if active may be able to reduce the expression of GAGE antigens, while the presence of MTs may actually increase the presence of several GAGE antigens. Overall the role that MT-3 and MTs play in the regulation of GAGE antigens needs to be further evaluated. Since the GAGE antigens are normally expressed in immune privileged tissues their overexpression in tumors allows them to be targeted by immunotherapy treatments. These tumors though are highly heterogenic in terms of

which GAGE antigens are present. It appears as though MTs may only upregulate a subset of the family. Researchers may use the presence or absence of MTs to help pick which GAGE antigens would be most beneficial to target during immunotherapy.

APPENDICES

APPENDIX A

Abbreviations

°C	Degree Centigrade
BSA	Bovine Serum Albumin
Cd^{2+}	Cadmium
cDNA	Copy of DNA made from mRNA
Da	Dalton's
DMEM	Dulbecco's Modified Eagles' Media
DNA	Deoxyribonucleic Acid
ECM	Extracellular Matrix
EMT	Epithelial-to-Mesenchymal Transition
ER	Estrogen Receptor
MT	Metallothionein

MT-1E	Metallothionein-1E
MT-3	Metallothionein-3
mRNA	Messenger RNA
MRE	Metal Response Element
μM	Micromolar
μL	Microliter
μg	Microgram
mL	Milliliter
mM	Millimolar
ng	Nanogram
PCR	Polymerase Chain Reaction
RNA	Ribonucleic Acid
RT-PCR	Reverse Transcriptase Polymerase Chain Reaction
Thr	Threonine
TE	Tris-EDTA

TER   Transepithelial Resistance

RNA   Ribonucleic Acid

SD   Standard Deviation

SEM   Standard Error of the Mean

WT   Wild Type

Zn^{2+} Zinc

Supplemental Figures
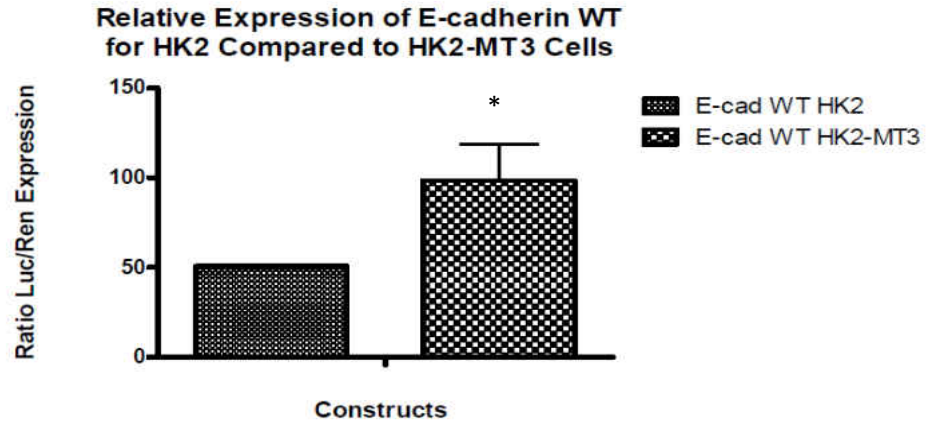
Supplemental Figure 23: Relative Expression of E-cadherin WT promoter for HK2 and HK2-MT-3 cells. The WT E-cadherin promoter construct was transfected into HK2 and HK2-MT-3 cell lines that are represented on the x axis. Data are expressed as a ratio of the Luciferase signal to the Renilla signal on the y axis. Statistical significance indicated by * P-value less than .05 as determined using the one-way ANOVA. Error bars represent SEM. Three biological replicates were tested.

Relative Expression of E-cadherin Mutant E-boxes for HK2 Compared to HK2-MT3 Cells
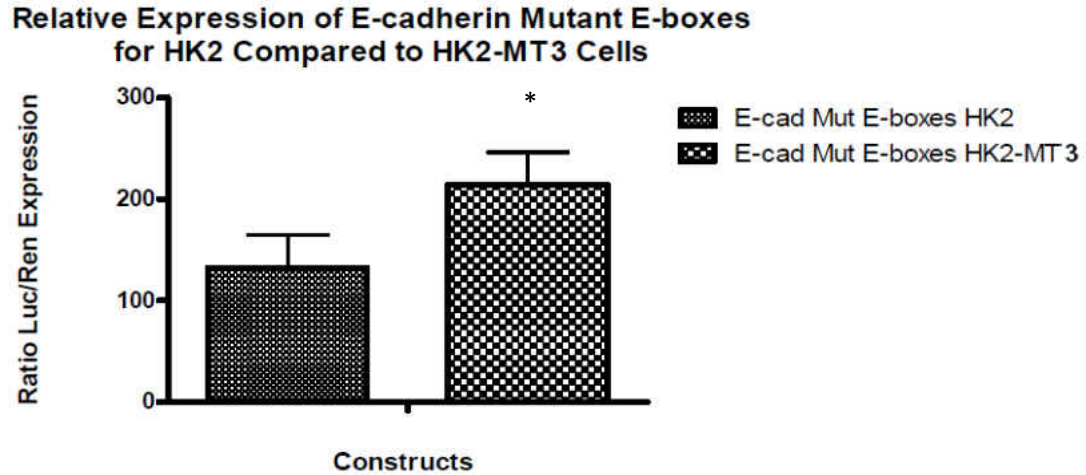
Supplemental Figure 24: Relative Expression of E-cadherin Mutant E-boxes promoter for HK2 and HK2-MT-3 cells. The E-cadherin promoter construct with mutated E-boxes was transfected into HK2 and HK2-MT-3 cell lines that are represented on the x axis. Data are expressed as a ratio of the Luciferase signal to the Renilla signal on the y axis. Statistical significance indicated by * P-value less than .05 as determined using the one-way ANOVA. Error bars represent SEM. Three biological replicates were tested.

AverageTER from Day 5 Post Seeding
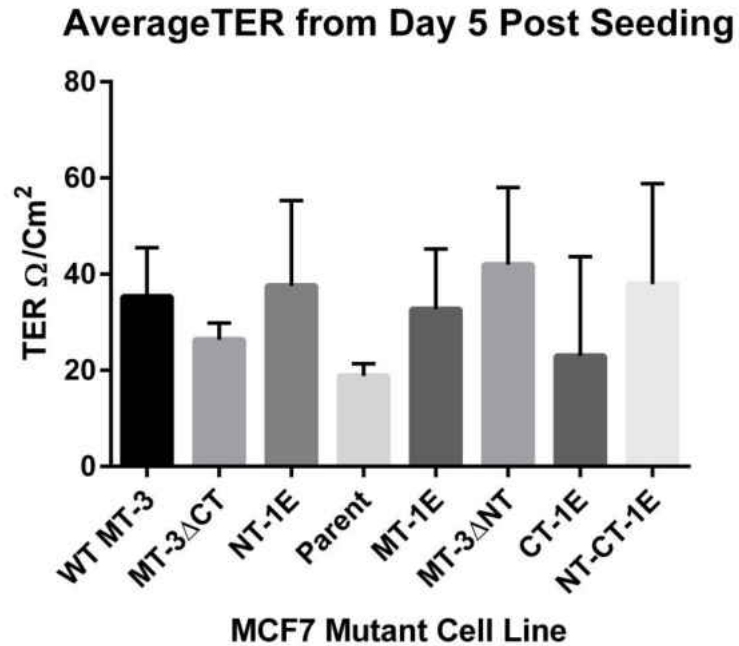
Supplemental Figure 25: **Average TER from Day 5 post seeding on trans-well**

inserts. Each MCF7 mutant cell line is represented on the x axis, while the calculated

TER is displayed on the y axis. Increased TER is indicative of the formation of tight

junctions, and is associated with the doming phenotype. Error bars represent SD. Three

biological replicates were tested.
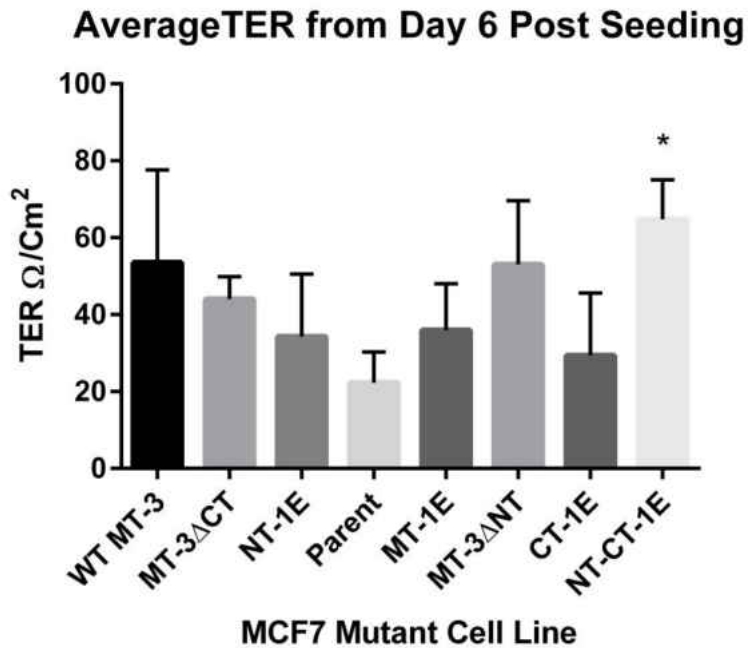
Supplemental Figure 26: **Average TER from day 6 post seeding on trans-well inserts.** Each MCF7 mutant cell line is represented on the x axis, while the calculated TER is displayed on the y axis. Increased TER is indicative of the formation of tight junctions, and is associated with the doming phenotype. Statistical significance indicated by * P-value less than .05 using the one-way ANOVA test and Dunnet's posttest for multiple comparisons using the MCF7 parent cell line as a control. Error bars represent SD. Three biological replicates were tested.

AverageTER from Day 7 Post Seeding
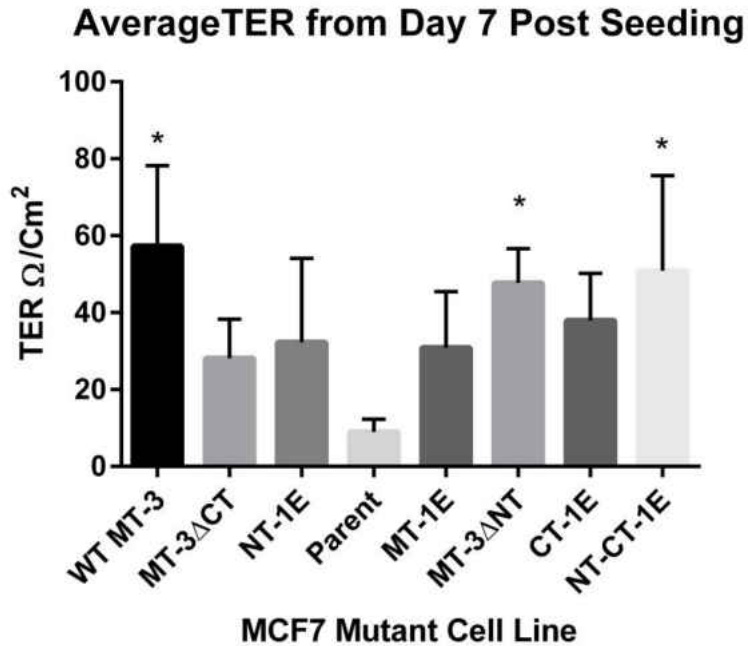
Supplemental Figure 27: **Average TER from day 7 post seeding on trans-well**

inserts. Each MCF7 mutant cell line is represented on the x axis, while the calculated

TER is displayed on the y axis. Increased TER is indicative of the formation of tight

junctions, and is associated with the doming phenotype. Statistical significance indicated

by * P-value less than .05 using the one-way ANOVA test and Dunnet's posttest for

multiple comparisons using the MCF7 parent cell line as a control. Error bars represent

SD. Three biological replicates were tested.

References

MCF7 ATCC ® HTB-22™ Homo sapiens mammary gland, breast; deri [Internet] [cited 2015 7/6/2015]. Available from: http://www.atcc.org/products/all/HTB-22.aspx#specifications .

Abbadi S, Rodarte JJ, Abutaleb A, Lavell E, Smith CL, Ruff W, Schiller J, Olivi A, Levchenko A, Guerrero-Cazares H, et al. 2014. Glucose-6-phosphatase is a key metabolic regulator of glioblastoma invasion. Mol Cancer Res .

Albrecht AL, Singh RK, Somji S, Sens MA, Sens DA, Garrett SH. 2008. Basal and metal-induced expression of metallothionein isoform 1 and 2 genes in the RWPE-1 human prostate epithelial cell line. J Appl Toxicol 28(3):283-93.

Andrews GK. 2000. Regulation of metallothionein gene expression by oxidative stress and metal ions. Biochem Pharmacol 59(1):95-104.

Antila E, Mussalo-Rauhamaa H, Kantola M, Atroshi F, Westermarck T. 1996. Association of cadmium with human breast cancer. Sci Total Environ 186(3):251-6.

Aschner M, Cherian MG, Klaassen CD, Palmiter RD, Erickson JC, Bush AI. 1997. Metallothioneins in brain--the role in physiology and pathology. Toxicol Appl Pharmacol 142(2):229-42.

Bathula CS, Garrett SH, Zhou XD, Sens MA, Sens DA, Somji S. 2008. Cadmium, vectorial active transport, and MT-3-dependent regulation of cadherin expression in human proximal tubular cells. Toxicol Sci 102(2):310-8.

Batlle E, Sancho E, Franci C, Dominguez D, Monfar M, Baulida J, Garcia De Herreros A. 2000. The transcription factor snail is a repressor of E-cadherin gene expression in epithelial tumour cells. Nat Cell Biol 2(2):84-9.

Bernstein L, Yuan JM, Ross RK, Pike MC, Hanisch R, Lobo R, Stanczyk F, Gao YT, Henderson BE. 1990. Serum hormone levels in pre-menopausal chinese women in shanghai and white women in los angeles: Results from two breast cancer case-control studies. Cancer Causes Control 1(1):51-8.

Biggs PJ, Warren W, Venitt S, Stratton MR. 1993. Does a genotoxic carcinogen contribute to human breast cancer? the value of mutational spectra in unravelling the aetiology of cancer. Mutagenesis 8(4):275-83.

Bremner I. 1991. Nutritional and physiologic significance of metallothionein. Methods Enzymol 205:25-35.

Cherian MG, Jayasurya A, Bay BH. 2003. Metallothioneins in human tumors and potential roles in carcinogenesis. Mutat Res 533(1-2):201-9.

Cheung IY, Chi SN, Cheung NK. 2000. Prognostic significance of GAGE detection in bone marrows on survival of patients with metastatic neuroblastoma. Med Pediatr Oncol 35(6):632-4.

Cilensek ZM, Yehiely F, Kular RK, Deiss LP. 2002. A member of the GAGE family of tumor antigens is an anti-apoptotic gene that confers resistance to fas/CD95/APO-1, interferon-gamma, taxol and gamma-irradiation. Cancer Biol Ther 1(4):380-7.

Claude P. 1978. Morphological factors influencing transepithelial permeability: A model for the resistance of the zonula occludens. J Membr Biol 39(2-3):219-32.

Cohen LA, Kendall ME, Zang E, Meschter C, Rose DP. 1991. Modulation of N-nitrosomethylurea-induced mammary tumor promotion by dietary fiber and fat. J Natl Cancer Inst 83(7):496-501.

Cousins RJ. 1983. Metallothionein--aspects related to copper and zinc metabolism. J Inherit Metab Dis 6 Suppl 1:15-21.

Czupryn M, Brown WE, Vallee BL. 1992. Zinc rapidly induces a metal response element-binding factor. Proc Natl Acad Sci U S A 89(21):10395-9.

De Backer O, Arden KC, Boretti M, Vantomme V, De Smet C, Czekay S, Viars CS, De Plaen E, Brasseur F, Chomez P, et al. 1999. Characterization of the GAGE genes that are expressed in various human cancers and in normal testis. Cancer Res 59(13):3157-65.

De Souza Santos E, De Bessa SA, Netto MM, Nagai MA. 2008. Silencing of LRRC49 and THAP10 genes by bidirectional promoter hypermethylation is a frequent event in breast cancer. Int J Oncol 33(1):25-31.

de Waard F and Baanders-van Halewijn EA. 1974. A prospective study in general practice on breast-cancer risk in postmenopausal women. Int J Cancer 14(2):153-60.

Ding ZC, Ni FY, Huang ZX. 2010. Neuronal growth-inhibitory factor (metallothionein-3): Structure-function relationships. FEBS J 277(14):2912-20.

Dutta R, Sens DA, Somji S, Sens MA, Garrett SH. 2002. Metallothionein isoform 3 expression inhibits cell growth and increases drug resistance of PC-3 prostate cancer cells. Prostate 52(2):89-97.

Favaro E, Bensaad K, Chong MG, Tennant DA, Ferguson DJ, Snell C, Steers G, Turley H, Li JL, Gunther UL, et al. 2012. Glucose utilization via glycogen phosphorylase sustains proliferation and prevents premature senescence in cancer cells. Cell Metab 16(6):751-64.

Garcia-Morales P, Saceda M, Kenney N, Kim N, Salomon DS, Gottardis MM, Solomon HB, Sholler PF, Jordan VC, Martin MB. 1994. Effect of cadmium on estrogen receptor levels and estrogen-induced responses in human breast cancer cells. J Biol Chem 269(24):16896-901.

Garrett SH, Sens MA, Todd JH, Somji S, Sens DA. 1999. Expression of MT-3 protein in the human kidney. Toxicol Lett 105(3):207-14.

Garrett SH, Phillips V, Somji S, Sens MA, Dutta R, Park S, Kim D, Sens DA. 2002. Transient induction of metallothionein isoform 3 (MT-3), c-fos, c-jun and c-myc in human proximal tubule cells exposed to cadmium. Toxicol Lett 126(1):69-80.

Gjerstorff MF and Ditzel HJ. 2008. An overview of the GAGE cancer/testis antigen family with the inclusion of newly identified members. Tissue Antigens 71(3):187-92.

Gjerstorff MF, Kock K, Nielsen O, Ditzel HJ. 2007. MAGE-A1, GAGE and NY-ESO-1 cancer/testis antigen expression during human gonadal development. Hum Reprod 22(4):953-60.

Gjerstorff MF, Johansen LE, Nielsen O, Kock K, Ditzel HJ. 2006. Restriction of GAGE protein expression to subpopulations of cancer cells is independent of genotype and may limit the use of GAGE proteins as targets for cancer immunotherapy. Br J Cancer 94(12):1864-73.

Gumulec J, Masarik M, Krizkova S, Adam V, Hubalek J, Hrabeta J, Eckschlager T, Stiborova M, Kizek R. 2011. Insight to physiology and pathology of zinc(II) ions and their actions in breast and prostate carcinoma. Curr Med Chem 18(33):5041-51.

Gurel V, Sens DA, Somji S, Garrett SH, Nath J, Sens MA. 2003. Stable transfection and overexpression of metallothionein isoform 3 inhibits the growth of MCF-7 and Hs578T cells but not that of T-47D or MDA-MB-231 cells. Breast Cancer Res Treat 80(2):181-91.

Hainaut P and Milner J. 1993. A structural role for metal ions in the "wild-type" conformation of the tumor suppressor protein p53. Cancer Res 53(8):1739-42.

Henderson BE, Ross RK, Pike MC, Casagrande JT. 1982. Endogenous hormones as a major factor in human cancer. Cancer Res 42(8):3232-9.

Henderson BE, Casagrande JT, Pike MC, Mack T, Rosario I, Duke A. 1983. The epidemiology of endometrial cancer in young women. Br J Cancer 47(6):749-56.

Hill J and Hodsdon W. 2014. In utero exposure and breast cancer development; an epigenetic perspective. Journal of Environmental Pathology, Toxicology and Oncology .

Jemal A, Thomas A, Murray T, Thun M. 2002. Cancer statistics, 2002. CA Cancer J Clin 52(1):23-47.

Kagi JH and Hunziker P. 1989. Mammalian metallothionein. Biol Trace Elem Res 21:111-8.

Kang SB, Marchelletta RR, Penrose H, Docherty MJ, McCole DF. 2015. A comparison of linaclotide and lubiprostone dosing regimens on ion transport responses in human colonic mucosa. Pharmacol Res Perspect 3(2):e00128.

Karin M, Haslinger A, Holtgreve H, Richards RI, Krauter P, Westphal HM, Beato M. 1984. Characterization of DNA sequences through which cadmium and glucocorticoid hormones induce human metallothionein-IIA gene. Nature 308(5959):513-9.

Khan S, Shukla S, Sinha S, Lakra AD, Bora HK, Meeran SM. 2015. Centchroman suppresses breast cancer metastasis by reversing epithelial–mesenchymal transition via downregulation of HER2/ERK1/2/MMP-9 signaling. Int J Biochem Cell Biol 58:1 <last_page> 16.

Kim DH, Roh YG, Lee HH, Lee SY, Kim SI, Lee BJ, Leem SH. 2013. The E2F1 oncogene transcriptionally regulates NELL2 in cancer cells. DNA Cell Biol 32(9):517-23.

Kobayashi Y, Higashi T, Nouso K, Nakatsukasa H, Ishizaki M, Kaneyoshi T, Toshikuni N, Kariyama K, Nakayama E, Tsuji T. 2000. Expression of MAGE, GAGE and BAGE genes in human liver diseases: Utility as molecular markers for hepatocellular carcinoma. J Hepatol 32(4):612-7.

Kong U, Koo J, Choi K, Park J, Chang H. 2004. The expression of GAGE gene can predict aggressive biologic behavior of intestinal type of stomach cancer. Hepatogastroenterology 51(59):1519-23.

Koumura A, Hamanaka J, Shimazawa M, Honda A, Tsuruma K, Uchida Y, Hozumi I, Satoh M, Inuzuka T, Hara H. 2009. Metallothionein-III knockout mice aggravates the neuronal damage after transient focal cerebral ischemia. Brain Res 1292:148-54.

Lacroix M and Leclercq G. 2004. Relevance of breast cancer cell lines as models for breast tumours: An update. Breast Cancer Res Treat 83(3):249-89.

Lee SJ and Koh JY. 2010. Roles of zinc and metallothionein-3 in oxidative stress-induced lysosomal dysfunction, cell death, and autophagy in neurons and astrocytes. Mol Brain 3(1):30,6606-3-30.

Levenson AS and Jordan VC. 1997. MCF-7: The first hormone-responsive breast cancer cell line. Cancer Res 57(15):3071-8.

Lever Julia eA. 1985. The culture of epithelial cells. plenum press, new york, NY. 1985. Plenum Press, New York, NY. .

Maeda K, Matsuhashi S, Tabuchi K, Watanabe T, Katagiri T, Oyasu M, Saito N, Kuroda S. 2001. Brain specific human genes, NELL1 and NELL2, are predominantly expressed in neuroblastoma and other embryonal neuroepithelial tumors. Neurol Med Chir (Tokyo) 41(12):582,8; discussion 589.

Maret W. 2004. Zinc and sulfur: A critical biological partnership. Biochemistry 43(12):3301-9.

Miles AT, Hawksworth GM, Beattie JH, Rodilla V. 2000. Induction, regulation, degradation, and biological significance of mammalian metallothioneins. Crit Rev Biochem Mol Biol 35(1):35-70.

Oren M and Prives C. 1996. p53: Upstream, downstream and off stream. review of the 8th p53 workshop (dundee, july 5-9, 1996). Biochim Biophys Acta 1288(3):R13-9.

Pablo JL and Pitt GS. 2014. Fibroblast growth factor homologous factors: New roles in neuronal health and disease. Neuroscientist .

Pratt SE and Pollak MN. 1993. Estrogen and antiestrogen modulation of MCF7 human breast cancer cell proliferation is associated with specific alterations in accumulation of insulin-like growth factor-binding proteins in conditioned media. Cancer Res 53(21):5193-8.

Quaife CJ, Kelly EJ, Masters BA, Brinster RL, Palmiter RD. 1998. Ectopic expression of metallothionein-III causes pancreatic acinar cell necrosis in transgenic mice. Toxicol Appl Pharmacol 148(1):148-57.

Rockhill B, Willett WC, Hunter DJ, Manson JE, Hankinson SE, Spiegelman D, Colditz GA. 1998. Physical activity and breast cancer risk in a cohort of young women. J Natl Cancer Inst 90(15):1155-60.

Ross-Innes CS, Stark R, Teschendorff AE, Holmes KA, Ali HR, Dunning MJ, Brown GD, Gojis O, Ellis IO, Green AR, et al. 2012. Differential oestrogen receptor binding is associated with clinical outcome in breast cancer. Nature 481(7381):389-93.

Roy DM and Walsh LA. 2014. Candidate prognostic markers in breast cancer: Focus on extracellular proteases and their inhibitors. Breast Cancer (Dove Med Press) 6:81-91.

Ruttkay-Nedecky B, Nejdl L, Gumulec J, Zitka O, Masarik M, Eckschlager T, Stiborova M, Adam V, Kizek R. 2013. The role of metallothionein in oxidative stress. Int J Mol Sci 14(3):6044-66.

Salomon AR, Ficarro SB, Brill LM, Brinker A, Phung QT, Ericson C, Sauer K, Brock A, Horn DM, Schultz PG, et al. 2003. Profiling of tyrosine phosphorylation pathways in human cells using mass spectrometry. Proc Natl Acad Sci U S A 100(2):443-8.

Samson SL and Gedamu L. 1998. Molecular analyses of metallothionein gene regulation. Prog Nucleic Acid Res Mol Biol 59:257-88.

Schmid KW, Ellis IO, Gee JM, Darke BM, Lees WE, Kay J, Cryer A, Stark JM, Hittmair A, Ofner D. 1993. Presence and possible significance of immunocytochemically demonstrable metallothionein over-expression in primary invasive ductal carcinoma of the breast. Virchows Arch A Pathol Anat Histopathol 422(2):153-9.

Sens MA, Somji S, Garrett SH, Beall CL, Sens DA. 2001. Metallothionein isoform 3 overexpression is associated with breast cancers having a poor prognosis. Am J Pathol 159(1):21-6.

Sewell AK, Jensen LT, Erickson JC, Palmiter RD, Winge DR. 1995. Bioactivity of metallothionein-3 correlates with its novel beta domain sequence rather than metal binding properties. Biochemistry 34(14):4740-7.

Shan B, Dong M, Tang H, Wang N, Zhang J, Yan C, Jiao X, Zhang H, Wang C. 2014. Voltage-gated sodium channels were differentially expressed in human normal prostate, benign prostatic hyperplasia and prostate cancer cells. Oncol Lett 8(1):345-50.

Simpson AJ, Caballero OL, Jungbluth A, Chen YT, Old LJ. 2005. Cancer/testis antigens, gametogenesis and cancer. Nat Rev Cancer 5(8):615-25.

Smyth GK. 2004. Linear models and empirical bayes methods for assessing differential expression in microarray experiments. Stat Appl Genet Mol Biol 3:Article3.

Somji S, Garrett SH, Zhou XD, Zheng Y, Sens DA, Sens MA. 2010. Absence of metallothionein 3 expression in breast cancer is a rare, but favorable marker of outcome that is under epigenetic control. Toxicol Environ Chem 92(9):1673-95.

Soule HD, Vazguez J, Long A, Albert S, Brennan M. 1973. A human cell line from a pleural effusion derived from a breast carcinoma. J Natl Cancer Inst 51(5):1409-16.

Strimmer K. 2008. A unified approach to false discovery rate estimation. BMC Bioinformatics 9:303,2105-9-303.

Takahashi Y, Ogra Y, Suzuki KT. 2005. Nuclear trafficking of metallothionein requires oxidation of a cytosolic partner. J Cell Physiol 202(2):563-9.

Thirumoorthy N, Manisenthil Kumar KT, Shyam Sundar A, Panayappan L, Chatterjee M. 2007. Metallothionein: An overview. World J Gastroenterol 13(7):993-6.

Thornalley PJ and Vasak M. 1985. Possible role for metallothionein in protection against radiation-induced oxidative stress. kinetics and mechanism of its reaction with superoxide and hydroxyl radicals. Biochim Biophys Acta 827(1):36-44.

Tian ZQ, Xu YZ, Zhang YF, Ma GF, He M, Wang GY. 2013. Effects of metallothionein-3 and metallothionein-1E gene transfection on proliferation, cell cycle, and apoptosis of esophageal cancer cells. Genet Mol Res 12(4):4595-603.

Tsuji S, Kobayashi H, Uchida Y, Ihara Y, Miyatake T. 1992. Molecular cloning of human growth inhibitory factor cDNA and its down-regulation in alzheimer's disease. EMBO J 11(13):4843-50.

Uchida Y, Takio K, Titani K, Ihara Y, Tomonaga M. 1991. The growth inhibitory factor that is deficient in the alzheimer's disease brain is a 68 amino acid metallothionein-like protein. Neuron 7(2):337-47.

Xu Y, Liu X, Guo F, Ning Y, Zhi X, Wang X, Chen S, Yin L, Li X. 2012. Effect of estrogen sulfation by SULT1E1 and PAPSS on the development of estrogen-dependent cancers. Cancer Sci 103(6):1000-9.

Yadav L, Puri N, Rastogi V, Satpute P, Ahmad R, Kaur G. 2014. Matrix metalloproteinases and cancer - roles in threat and therapy. Asian Pac J Cancer Prev 15(3):1085-91.

Zambon A, Mandruzzato S, Parenti A, Macino B, Dalerba P, Ruol A, Merigliano S, Zaninotto G, Zanovello P. 2001. MAGE, BAGE, and GAGE gene expression in patients with esophageal squamous cell carcinoma and adenocarcinoma of the gastric cardia. Cancer 91(10):1882-8.

Zeng J, Vallee BL, Kagi JH. 1991. Zinc transfer from transcription factor IIIA fingers to thionein clusters. Proc Natl Acad Sci U S A 88(22):9984-8.